

REPORT DOCUMENTATION PAGE

*Form Approved
OMB No. 0704-0188*

The public reporting burden for this collection of information is estimated to average 1 hour per response, including the time for reviewing instructions, searching existing data sources, gathering and maintaining the data needed, and completing and reviewing the collection of information. Send comments regarding this burden estimate or any other aspect of this collection of information, including suggestions for reducing the burden, to the Department of Defense, Executive Services and Communications Directorate (0704-0188). Respondents should be aware that notwithstanding any other provision of law, no person shall be subject to any penalty for failing to comply with a collection of information if it does not display a currently valid OMB control number.

PLEASE DO NOT RETURN YOUR FORM TO THE ABOVE ORGANIZATION.

1. REPORT DATE (DD-MM-YYYY) 31 JAN 08			2. REPORT TYPE FINAL REPORT		3. DATES COVERED (From - To) 1 MAY 04 TO 31 MAR 07				
4. TITLE AND SUBTITLE NEUROMORPHIS MODELING OF MOVING TARGET DETECTION IN INSECTS				5a. CONTRACT NUMBER FA9550-04-1-0286					
				5b. GRANT NUMBER					
				5c. PROGRAM ELEMENT NUMBER 61102F					
				6. AUTHOR(S) DR PATRICK SHOEMAKER			5d. PROJECT NUMBER 2304		
							5e. TASK NUMBER TB		
							5f. WORK UNIT NUMBER		
7. PERFORMING ORGANIZATION NAME(S) AND ADDRESS(ES) TANNER RESEARCH, INC. 2650 EAST FOOTHILL BLVD. PASADENA, CA 91107				8. PERFORMING ORGANIZATION REPORT NUMBER					
9. SPONSORING/MONITORING AGENCY NAME(S) AND ADDRESS(ES) AFOSR/NL 875 NORTH RANDOLPH STREET SUITE 325, ROOM 3112 ARLINGTON, VA 2203-1768				10. SPONSOR/MONITOR'S ACRONYM(S)					
				11. SPONSOR/MONITOR'S REPORT NUMBER(S)					
12. DISTRIBUTION/AVAILABILITY STATEMENT APPROVED FOR PUBLIC RELEASE. DISTRIBUTION IS UNLIMITED				AFRL-SR-AR-TR-08-0063					
13. SUPPLEMENTARY NOTES									
14. ABSTRACT Ionic polymers under development fir use in wide-ranging applications from bio/chem sensing to remote robotics. SMA are being considered for chevron design to reduce jet noise and increase performance, as well as attenuation in modular antennas.									
15. SUBJECT TERMS									
16. SECURITY CLASSIFICATION OF:			17. LIMITATION OF ABSTRACT	18. NUMBER OF PAGES	19a. NAME OF RESPONSIBLE PERSON				
a. REPORT	b. ABSTRACT	c. THIS PAGE			19b. TELEPHONE NUMBER (Include area code)				

Grants FA9550-04-1-0283 and FA9550-04-1-0294

Neuromorphic Modeling of Moving Target Detection in Insects

Final Report

Patrick Shoemaker

Tanner Research, Inc.
2650 East Foothill Blvd.
Pasadena CA 91107
USA

20080213211

This report is copyright 2007.

DISTRIBUTION STATEMENT A. APPROVED FOR PUBLIC RELEASE; DISTRIBUTION IS UNLIMITED.

1. Objectives

The overall objective of our work has been to characterize and develop models for the processing associated with *Small Target Movement-Detecting* (STMD) neurons in insects, building on the results of our prior AFOSR research contract (F49620-01-C-0030).

Characterization, as the objective of the experimental neuroscience element of the work, proceeded with the twin goals of establishing a catalogue of basic physiological characteristics and a tentative classification of the various STMD types encountered; and throwing light on particular aspects of the computations underlying their response capabilities. Modeling and simulation were undertaken with the goal of understanding those computational mechanisms, including the contributions of various processing stages hypothesized to lie on the neural pathway leading to STMDs.

2. Summary and Final Status of Effort

2.1. Modeling and Simulation

Although the study of STMDs remains in its infancy and the goal of understanding their computational basis is not yet fully realized, our modeling efforts have helped to narrow our hypotheses and to direct the experimental questions that must be answered in further pursuit of the goal. In addition to STMD modeling, solid progress has been made in some new areas that were not anticipated at the start of the project – in particular, the modeling of rectifying transient cells as a possible STMD presursor, and the electrical properties of NMDA receptors as a neural mechanism for nonlinear facilitation. These new topics we believe will ultimately contribute to the understanding of STMDs.

At the commencement of the project, we posited a hierarchy of computational stages that was consistent with available data on STMDs. As experimental work proceeded, plausible and detailed models for some of these stages were elaborated only to be discounted by results from a subsequent experiment. In addition, other promising ideas were developed that could not be successfully generalized or tied to the electrophysiology. As the project progressed, the pursuit of alternative hypotheses led to the consideration of rectifying transient cells and NMDA-mediated electrical behavior in neurons. This new work has suggested that our hypothetical computational stages may not in fact correspond to a set of distinct processing elements, i.e., a succession of neuron types in the pathway leading to STMDs, although we still regard these stages as useful for conceptualizing the basic functional characteristics of STMD processing.

Beyond the primary goal, modeling and simulation have also proven useful and justified in their own right as a tool in support of electrophysiological research: experimental design has been guided to a significant degree by the testable hypotheses generated by modeling at both the conceptual and numerical levels.

Finally, silicon modeling – the implementation of STMD or related models in analog VLSI circuitry – was specified as an activity in the project proposal, but was de-emphasized during its execution in favor of more detailed development of biologically-based models. A single submission of two test die containing bio-inspired circuits was made to a DARPA-sponsored fabrication run of an experimental three-dimensional (three interconnected wafer tiers) integrated circuit process. Unfortunately, delays in the

completion of this fabrication have precluded test and evaluation of these circuits during the project, in spite of an extension of the period of performance of the grant.

2.1.1. Background

As noted, at the close of our prior AFOSR contract on STMD neurons we hypothesized a hierarchy of functional elements for STMD processing. This hierarchy may be summarized as follows:

1. Elementary motion detection: A fundamental and local computation that is distributed retinotopically across the entire visual field, and provides the ability to discriminate local motion cues from changes in luminance that are non-motion-related.
2. Longitudinal target size discrimination: The ability to discriminate 'smallness' of target in direction of motion. Such processing may serve to filter the outputs of elementary motion detectors for events consistent with passage of a small object.
3. Target / background speed discrimination: The capability to distinguish a moving target from a moving cluttered background (which may contain small features indistinguishable from 'targets'), on the basis of relative velocity.
4. Lateral target size discrimination: The ability to discriminate 'smallness' of target in the dimension perpendicular to direction of motion. This (along with enhancement of directional selectivity) was assumed to be a principal function of cells that we previously labeled Elementary Small Target Movement Detectors (ESTMDs).
5. Wide-field enhancement of small moving target selectivity: A postulated characteristic of wide-field STMD neurons that exploits the constraint of continuity of motion over some distance in the receptive field, in order to obtain more reliable, higher-confidence detection of small moving targets.

For each of these functions, we developed conceptual (and in most cases, computational) models during this prior effort. Following, we summarize these models:

1. Elementary motion detection: The *correlational* or *Reichardt EMD* model, or its constituent parts (i.e., correlator units), were regarded as the primary candidates for front-end processing.
2. Longitudinal target size discrimination: A model for this function was based on the detection of triphasic waves in the outputs of individual Reichardt EMDs. With proper pre-processing in the early visual pathway (i.e., 'imperfect' highpass temporal filtering), the presence of such waves was found to be an indicator of a longitudinally small target. A computational model was developed, based on gating the rectified response to the negative-going output phase by the local average of the output (which is net positive for a small target moving in the preferred direction).
3. Target / background speed discrimination: For this function, we postulated an element called a primitive small target movement detector (PSTMD). This model involves a comparison of the traversal across pairs of ommatidia of 'small target events' with the expected traversals of moving background. The comparison is achieved with an EMD-like element that is tunable by feedback representing the state of local background motion, which performs 'anticorrelations' of expected

and actual events (by the mechanism of shunting inhibition) rather than correlations. In this way, stimuli that are consistent with background motion are suppressed, while inconsistent events – e.g., the passage of a small target with a velocity different than background – elicit a response.

4. Lateral target size discrimination: For this function, we developed a series of models for the experimentally-observed characteristics of ESTMD neurons. These are based on a receptive field with a notched inhibitory surround and an excitatory center, and ‘tonic’ or slowly decaying responses in each region. Only when a target enters the receptive field via the notch, and is small enough laterally to fit through the notch, can the cell reach a net state of excitation. Silicon as well as computational models for this function were developed.
5. Wide-field enhancement of small moving target selectivity: For this function, we postulated a mechanism based on dendritic processing. Excitatory synapses from earlier processing elements such as ESTMDs are supposed to map onto dendrites of a wide-field cell in a retinotopic fashion, such that reinforcement of excitatory potentials occurs when ESTMDs are excited sequentially along continuous tracks in visual space. A silicon model was also developed for this processing.

The processing represented by these models was assumed to proceed hierarchically in the order above, in a series of stages associated with the neural pathway that extends between the retina and the lobula. This overall hierarchical model was guided by the assumption that successive steps should increasingly filter out events in the input signal that are inconsistent with small target motion relative to background. By largely eliminating responses due to flicker, to longitudinally extensive objects, and to background motion, the first three stages above reduce the probability that a non-small-target event can trigger a response, or inhibit response to an actual small target, in an ESTMD.

2.1.2. Simulation Methods and Data

Simulations of models for various stages of STMD processing were performed during the project. These included individual stages in isolation, and in other cases multiple stages cascaded in the order in which it is assumed they occur in the neural pathway. In all cases, input data corresponding to raw luminance histories were passed through a model for early visual processing prior to the models under investigation. Simulations generally comprised calculation of the time-domain response of a model system to sequences of stimuli. The model systems and stimuli covered a range of topologies and complexities, including some characterizing transient responses of a single stage or cascade of stages excited by a single input signal, some involving one-dimensional sensor/processor arrays with lateral interactions, with a small target moving against a stationary or moving linear background, and others using full two-dimensional arrays and input data, generated as described in Experimental Methods in Section 3. The data sequences for this last class included orbiting targets of two contrasts and sizes, against slower horizontal and vertical background motion, and are identified in this report by the labels ‘otlhcbtrs’ (orbiting target, large / high contrast, background rightward slower than target), ‘otlhcbds’ (orbiting target, large / high contrast, background downward slower than target), and ‘otslcbds’ (orbiting target, small / low contrast, background downward slower than target). The bulk of the simulations were performed with ‘otslcbds’ since it is the most challenging of the three scenarios. For these

simulations, data sampling and retinotopic arrays of processing elements were defined on a hexagonal lattice corresponding to the ommatidial geometry in the insect eye, and a retinotopic architecture was maintained through the level of the ESTMD.

In addition, during the latter part of the project, two-dimensional input data were generated corresponding to small targets fixed against natural backgrounds, to investigate responses when the background was animated and there was no relative motion between it and the targets themselves. In the earliest of these, data and processor arrays were defined on a rectangular lattice, but the models were subsequently transferred to a hexagonal geometry. The corresponding simulations primarily involved models for the rectifying transient cells and precursor processing.

Models were coded and simulations were performed using the tool SPICE (Simulation Program with Integrated Circuit Emphasis, as the product T-SPICE, Tanner Research, Monrovia, CA), and in the latter part of the project, MATLAB / Simulink (The Math Works, Natick, MA). Details of the imagery generation, data handling, and data interchange formats followed the conventions described in reports for our prior project F49620-01-C-0030.

2.1.3. *Early Vision (O'Carroll, Brinkworth, Shoemaker)*

During the project, we adopted a standard model for early visual processing that is consistent with the known properties of the compound eye optics, retina, and first optic ganglion (the lamina) in insects. This model involves no contribution of our own, but is based on prior work. A reasonable representation of early vision was regarded as important for the fidelity of simulations of subsequent processing. Similar processing was used in some of the simulations during the prior contract, but the current version was applied systematically to the input (i.e., luminance) data used in the present effort. We detail the model here as follows.

The geometrical optics of the model were scaled to reflect the approximate characteristics of the eyes of large, visually acute dipterans. The hexagonal grid was set up such that the orbiting target in the input scenarios subtends about 15 inter-ommatidial angles in visual space. This is a slightly closer view than would be observed by an insect mounted in the experimental stage in the laboratory, viewing the original full-size video projected on the CRT. Compound eye optics were modeled by blurring of relatively high-resolution input imagery by a Gaussian modulation transfer function F of the form

$$F(\phi) = \exp[-2.77\phi^2 / \sigma^2], \quad (1)$$

where ϕ is angular deviation from the optical centerline of an individual ommatidium, and the standard deviation σ was set to about 1.1 times the inter-ommatidial angle. Discrete spatial convolution with this function was performed on the original pixel grid during the process of resampling of the raw input data onto the hexagonal grid, in order to form input data for the simulations.

The early vision model included a linear lowpass temporal filter that reflects photoreceptor temporal response, with a transfer function (Laplace transform) $1/(\tau_L s + 1)$, where s is the Laplace variable, and where τ_L was set in the neighborhood of 3ms, corresponding to a corner frequency of about 53Hz. Following this, a Lipetz, or Naka-Rushton transformation was applied. This transformation is specified by the equation

$$U = I^a / (I^a + I_0^a), \quad (2)$$

where I is the input intensity, I_0 a parameter defining mid-response level, a is an exponent between 0.5 and 1, and U is the output. The exponent a was set to the value 0.7. In the first half of the project, the mid response level parameter I_0 was set to 120, which approximates the geometric mean of the 8-bit luminance data (range [0,255]) in the imagery used in simulations. In the latter part of the project, this parameter was varied by setting it to a low-pass-filtered version of the input luminance, with a time constant on the order of 1s, as a means of approximating luminance adaptation. Finally, a highpass temporal filter with transfer function (Laplace transform) $\tau_{HS}/(\tau_{HS}+I)$ was applied, where s is the Laplace variable, and where τ_H was set various values depending on the detail of the individual models to follow.

2.1.4. Elementary Motion Detection and the Correlational EMD (O'Carroll, Shoemaker)

Following up on work under the prior contract, we performed further simulations in which the correlational or Reichardt EMD was used in combination with detection of triphasic output signatures for elementary motion detection and longitudinal size discrimination. These included simulations using a detailed model of the EMD as implemented in silicon in the prior contract. This approach was abandoned for subsequent models including the Small Event Motion Detector and Rectifying Transient Cell models.

2.1.5. The Small Event Motion Detector (Shoemaker)

The *Small Event Motion Detector* (SEMD) model originated during the present grant. This element provides both elementary motion detection and selectivity for longitudinally small objects in a single unit. It is computationally similar to the standard correlational elementary motion detector (EMD) in that the fundamental operation is the product of input signals from neighboring ommatidia. In the SEMD, however, these input signals are first passed through a highpass filtering stage with a short time constant, so that the signals that are multiplied together reflect rapid transients. The multiplication operation is followed by half-wave rectification for the negative-going phase of the product. These operations select for transients that are of opposite sign at the two neighboring locations, and render the SEMD sensitive to the coincidence of a leading edge at one location and a trailing edge at another – an effective discriminant for the passage of a longitudinally small target. Because no delay function or other asymmetric temporal processing is associated with the two legs of the correlator, the response at any particular speed is maximal when the leading and trailing edges are exactly one pixel apart (i.e., the optimum target extent is one ommatidium). Another consequence of this symmetry is that the SEMD has no directional sensitivity – the response is the same if the direction of motion of a target is reversed. It does of course have orientation selectivity on a two-dimensional 'retina' by virtue of being aligned with some particular inter-ommatidial axis. There is one SEMD for each inter-ommatidial boundary in our model system.

During the first half of the project, considerable effort was directed toward development and evaluation of this model. Initially, it was simulated in isolation using synthetic input data corresponding to a moving pulse against a uniform background. Its basic operation was investigated, and the consistency of its joint target speed/size tuning

with the characteristics of biological STMD neurons was demonstrated. A suite of more realistic simulations was then performed to further characterize it and compare its results to neurobiological data from STMD cells. We studied the effects of varying the tuning and topology (i.e., time constant and order) of the highpass filter, in simulations of single units and small subarrays. These simulations used segments of the orbiting target datasets, each containing a target transit in one direction, or background motion only, and employed the standard early vision model of Section 2.1.3 above. Following these simulations, a 'standard' version of the SEMD was selected and simulated for the various complete orbiting target scenarios in a full-size (31x31 hexel) array. The model was ultimately abandoned following electrophysiological experiments to test its predictions, and attention focused on the rectifying transient cells.

2.1.6. The Primitive Small Target Movement Detector (Shoemaker)

The *Primitive Small Target Movement Detector* (PSTMD), originated during the prior contract, is intended to discriminate target from background motion on the basis of relative velocity. Its operation involves a comparison of local events with the expected traversal of moving background. The comparison is achieved with an EMD-like element that is excited by local input, and is also subject to shunting inhibition by a delayed signal passed from a nearby unit. In the original version of the PSTMD, the delayed signal was simply derived from the input signal of a single nearby PSTMD, and the delay operator was a lowpass filter. This delayed signal represents the estimate of background motion, and the delay time is tuned to reflect the speed of that motion. The shunting inhibition is modeled with a division, with a small constant term in the denominator representing the inverse of the maximum gain for the unit. The inhibition is intended to suppress responses to moving background events, but to leave the PSTMD responsive to events inconsistent with the background motion, i.e., the passage of a small target with a different velocity. We performed simulations of the PSTMD concept using the arrays developed in the prior project, but with inputs to PSTMDs supplied by SEMDs rather than correlational EMDs or synthetic input signals as used in prior work. The SEMDs were excited by input segments derived from the orbiting target scenarios (some including target transit and some, background motion alone to test rejection of background motion). In our model system, a full complement of PSTMDs would include one pair for each SEMD (i.e., one for each direction along each inter-ommatidial axis).

Simulations with the original model and several variants confirmed or revealed a number of shortcomings of the approach (discussed in 'Accomplishments / New Findings' in Section 3.1.3 below), including in particular the inability to distinguish target from background motion when the velocities are at all similar. As a result we undertook a major revision of the PSTMD model during the present grant.

In this revision, we developed the notion of a 'propagating predictor' for background motion. This involves a retinotopic network with spatial as well as temporal memory, in which estimates of SEMD responses to background motion are passed to a 'neuron' from its neighbor(s), reinforced by any local SEMD input, and then delayed and passed on. Because the local estimate of background motion is dependent on its history across a region of the network, and not just at one neighboring unit, we expected this approach to be capable of a more accurate estimate of background events with less influence due to a target that is moving with a velocity similar to the background (assuming that the delay in

the network is tuned to match the local speed of propagation). This method is related to a target-tracking algorithm developed by T. Bartolac at Tanner Research and called the 'Wave Process' (Bartolac and McCarley, 2003), which involves propagation of waves in a two-dimensional discrete network and the reinforcement of those waves by input from a moving stimulus. Our version is biologically plausible and could be realized in a neural network.

This PSTMD model was developed initially in one-dimensional form and simulated using input data segments extracted from columns of the orbiting target dataset (some containing a target transit and some containing only background motion). Simulations included early vision and SEMD processing as well. Encouraging results were obtained in the one-dimensional case, and we attempted with considerably less success to generalize the concept to a two-dimensional retinotopic network.

During the latter part of the grant, work on the PSTMD was put on hold due to electrophysiological experiments suggesting the importance of small target spatial statistics for discrimination in biological STMDs, and the apparent difficulty that they have discriminating same-direction target and background motion.

2.1.7. *The Elementary Small Target Motion Detector (Shoemaker, O'Carroll)*

Models for the *Elementary Small Target Motion Detector* (ESTMD) were first developed during the prior grant, and in contrast with the SEMD and PSTMD, are based on the observed characteristics of a class of neurons that have been encountered and characterized electrophysiologically in the past – the cells also labeled ESTMDs. As an element in our proposed processing hierarchy, ESTMD models provide lateral target size discrimination as well as imparting or enhancing directional selectivity. These are based on a receptive field with a notched inhibitory surround and an excitatory center, and 'tonic' or persistent responses in each region. The fundamental idea is that only when a target enters the receptive field via the notch, and is small enough laterally to fit through the notch, is the cell able reach a net state of excitation. ESTMDs in our prior work were arranged in hexagonal arrays, with a one-unit excitatory center and five of the six surrounding units defining the notched inhibitory surround. Input data were synthetic (i.e., not derived from any prior visual motion processing stages).

Modeling and simulation of the ESTMD during the current grant focused initially on the 'tonic' temporal element that is responsible for the nonlinear dynamic behavior of the overall model. We developed a concept (demonstrated in a *silicon* model near the end of the prior effort) in which rapid activation is followed by a 'sustained tonic' response rather than slow decay of the output that commences immediately after stimulation. We expected this characteristic would ultimately allow the ESTMD model to discriminate more unambiguously between preferred- and non-preferred-direction moving stimuli.

After work on this temporal model, a complete ESTMD was formulated with inputs derived from prior motion processing stages for the first time. These ESTMDs receive inputs directly from SEMDs (PSTMDs were not included due to lack of success in formulating two-dimensional architectures). Receptive fields are larger than in the prior work, but as before contain inhibitory and excitatory regions, with each showing persistent behavior, and with the 'notch' in the inhibitory subfield implemented by an asymmetric pattern of connections from inhibitory 'interneurons' onto the ESTMD output unit.

2.1.8. Rectifying Transient Cells (Shoemaker, Wiederman)

By the halfway point of the project, pilot experiments on STMD neurons with new experimental protocols had provided feedback on some of the hypotheses involved in the models described above. Particularly for the processing elements for which no neural correlates have been observed electrophysiologically (i.e., the SEMD and PSTMD), the new data made clear just how speculative various aspects of these models are, leading to a reassessment of the overall approach: while continued development of 'bio-inspired' models might lead to new algorithms for small target detection and tracking, their value in understanding details of the processing in the biological system is limited until detailed physiological evidence can be applied to test their key features. This provided motivation for development of further test protocols, and especially for the identification, investigation, and modeling of other possible neural elements in the STMD pathway.

For this reason, modeling and simulation at the level of the STMD was relatively limited during the last half of the project. We instead pursued an interest in the *Rectifying Transient Cells* as a possible precursor to the STMD. Initial modeling efforts were based on previously reported results (Jansonius and van Hateren, 1991, 1993; Osorio, 1987) and predated our own electrophysiological work on such cells. We developed a basic model for the lamina neurons of this class (the 'on-off' cells of Jansonius and van Hateren, 1991, 1993), focusing primarily on the full-wave rectifying nonlinearity and temporal characteristics (i.e., fast adaptation). Separate ON and OFF processing channels with independent adaptation were proposed, in work done primarily by the industrial partner. Subsequently, as experimental work commenced, the model was elaborated with detailed spatial interactions added to its temporal features in work by the academic partner. The model was then applied to small target data, with targets moving at the same velocity as a cluttered background, to demonstrate the salience of small target spatial characteristics in RTC response. These results have given us reason to believe that we may finally have identified a relevant stage of precursor processing for the STMD, and will be able to apply electrophysiological data from these cells in order to develop a more successful and biologically grounded STMD model.

2.1.9. Dendritic Spatiotemporal Processing

Dendritic spatiotemporal processing has been postulated to enhance the reliability and selectivity for small moving targets in wide-field STMDs. Excitatory synapses from earlier processing elements, such as ESTMDs, are supposed to map onto dendrites of a wide-field cell in a retinotopic fashion, such that reinforcement of excitatory potentials occurs when ESTMDs are excited sequentially along continuous tracks in visual space.

An abstract computational model and a silicon implementation were developed for this type of processing during the prior contract, but efforts under the current grant have been limited to consideration of biophysical mechanisms for the nonlinear facilitation that would underlie the hypothesized function. This led to work on the implications of a particular nonlinear synaptic receptor conductance, as described in the following section.

2.1.10. NMDA Receptors and Bistable / Amplifying Neural Behavior (Shoemaker)

NMDA receptors are a class of metabotropic or second-messenger synaptic receptors that are typically activated *in vivo* by the neurotransmitter glutamate, with N-methyl-D-aspartate (NMDA) acting as a specific agonist. The current/voltage relationship of NMDA receptor ion channels is significantly nonlinear under physiological conditions, which can give rise to bistable and facilitatory behavior in neurons and neural structures. Such behavior could provide a biophysical substrate for the sort of nonlinear facilitation envisioned for dendritic spatiotemporal processing as mentioned above, and indeed for the fundamental nonlinearity underlying directional motion detection itself.

In the last nine months of the project, we analyzed the conditions under which bistable regimes of operation prevail in neurons and dendrites, and also general amplifying properties, due to NMDA receptors in concert with other membrane conductances. We considered primarily the case in which other conductances are nearly ohmic in nature; these include a number of important synaptic conductances such as AMPA, GABA_A, and GABA_B receptors. The methodology consisted of numerical and mathematical analyses of both single electrical compartments and cable-like dendrites with proximal somatic loads, with NMDA and other conductances present in the membrane. One product of this work is models for compartments and dendrites that can be used to implement NMDA-based computational primitives in further simulations.

2.1.11. Silicon Modeling (Shoemaker)

The DARPA-sponsored experimental three-dimensional IC process (3DM2) involves stacking of multiple wafers (three layers at present), with electrical contacts between wafers, in a silicon-on-insulator process developed at MIT / Lincoln Laboratory. This makes it a very promising medium for direct implementation of the sensor-parallel, layer-serial architecture that is natural for neuromorphic sensory processing. We developed visual motion detection circuitry, including photodetectors, early vision, and models for both rectifying transient cells and correlational EMDs. The final version of these circuits were submitted to fabrication on 4 NOV 2006, but were not received back before termination of the present grant.

3. Accomplishments / New Findings

3.1. Modeling and Simulation

3.1.1. Elementary Motion Detection and Longitudinal Size Discrimination (O'Carroll, Shoemaker)

When a circuit-based model for the correlational EMD was simulated in response to synthetic small targets, we found that the triphasic output signatures could be obtained, as in prior simulations with biologically-based models. This result required proper configuration and tuning of the early vision filtering (i.e., an imperfect highpass characteristic that passes some DC component), and we found that it was not particularly robust with respect to variations in the model parameters and the characteristics of the synthetic target. Thus, detection of longitudinally small moving features based on this signature was judged to be a problematic approach (particularly for a VLSI model), and this result motivated the investigation of alternative approaches to modeling the function of longitudinal target size discrimination.

3.1.2. The Small Event Motion Detector (Shoemaker)

The SEMD represents an attempt to develop a more robust model for both elementary motion detection and longitudinal size discrimination that (at its conception) was also consistent with the electrophysiological data available. As noted, the model is computationally similar to the standard correlational EMD: the fundamental operation is the correlation (product) of input signals from neighboring ommatidia. The SEMD, however, is preceded by a highpass filtering stage with a short time constant, so that the prefiltered inputs produced by this stage reflect rapid transients. In addition, the correlation operation is followed by half-wave rectification for the negative-going phase of the product. These operations select for transients which at any instant are of opposite sign at the two neighboring locations, and render the SEMD sensitive to the coincidence of a leading edge at one location and a trailing edge at another – an effective discriminant for the passage of a longitudinally small target. Thus selectivity for longitudinal smallness is made an inherent part of an elementary motion detection operation.

Basic Response Characteristics of the SEMD

The response of an SEMD to synthetic targets is illustrated in Figure 1 along with its prefiltered inputs to give some intuition with respect to its operation. The top graph illustrates the inputs and output of an SEMD in response to a moving target (consisting of a square pulse of greater luminance than a uniform background) whose longitudinal extent is equivalent to the inter-ommatidial separation. The bottom graph illustrates the response of the same SEMD to a target whose longitudinal extent is four times the interommatidial distance.

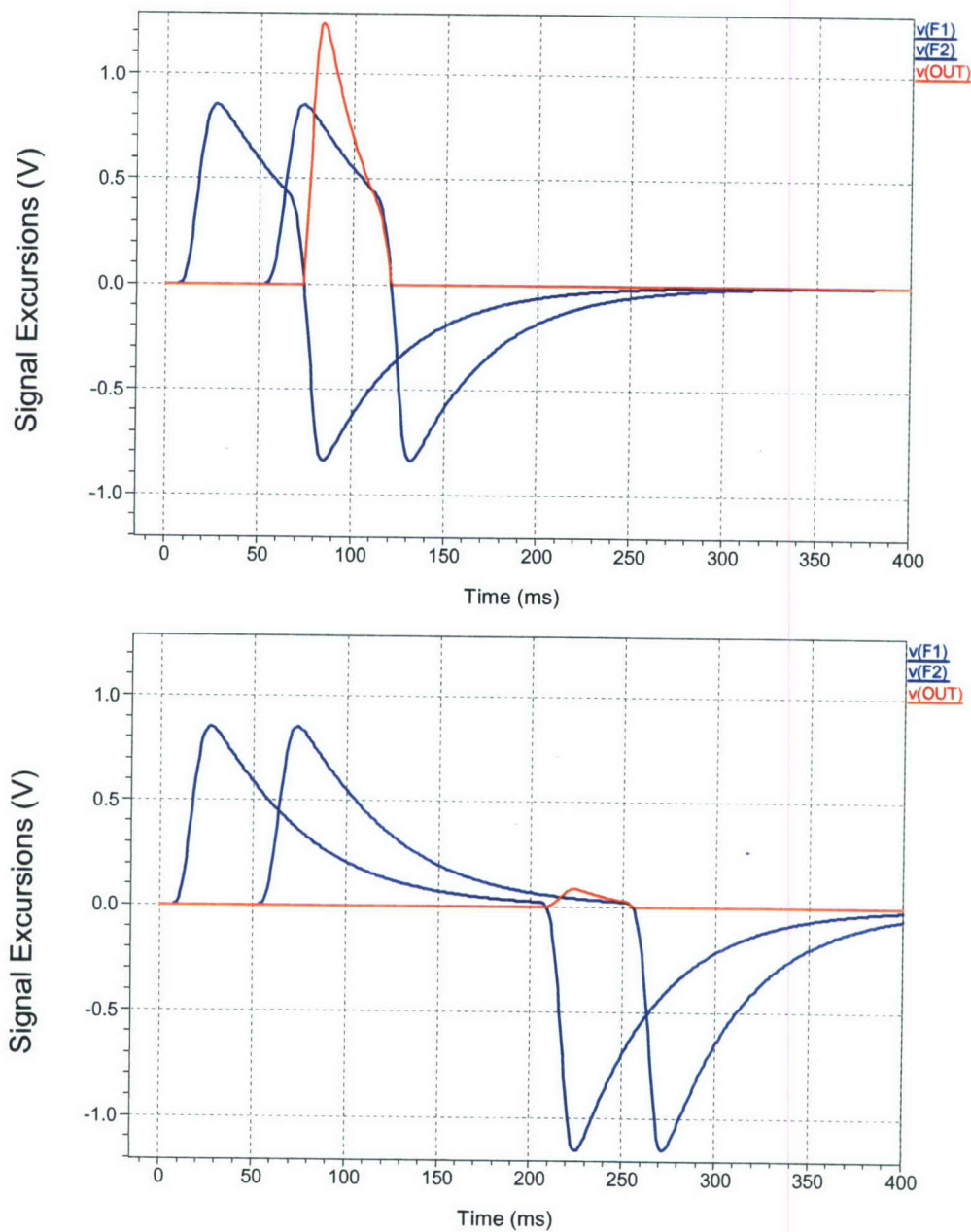


Figure 1: Response of an SEMD to the passage of a small moving target 1.5° in longitudinal extent (top) and 6° in longitudinal extent (bottom). The interommatidial angle is 1.5° and the target speed $32^\circ/\text{s}$ in both cases. The first or ‘upstream’ input to the SEMD is shown in dark blue, the second or ‘downstream’ input in lighter blue, and the output in red. The time constant of the highpass prefilter is set to 40ms in both cases.

The spatiotemporal tuning of the SEMD was characterized in simulations by recording its peak output as a function of target speed and longitudinal extent. This tuning is

remarkably similar to that observed in biological STMD neurons, with peak response occurring at higher speeds for longer targets.

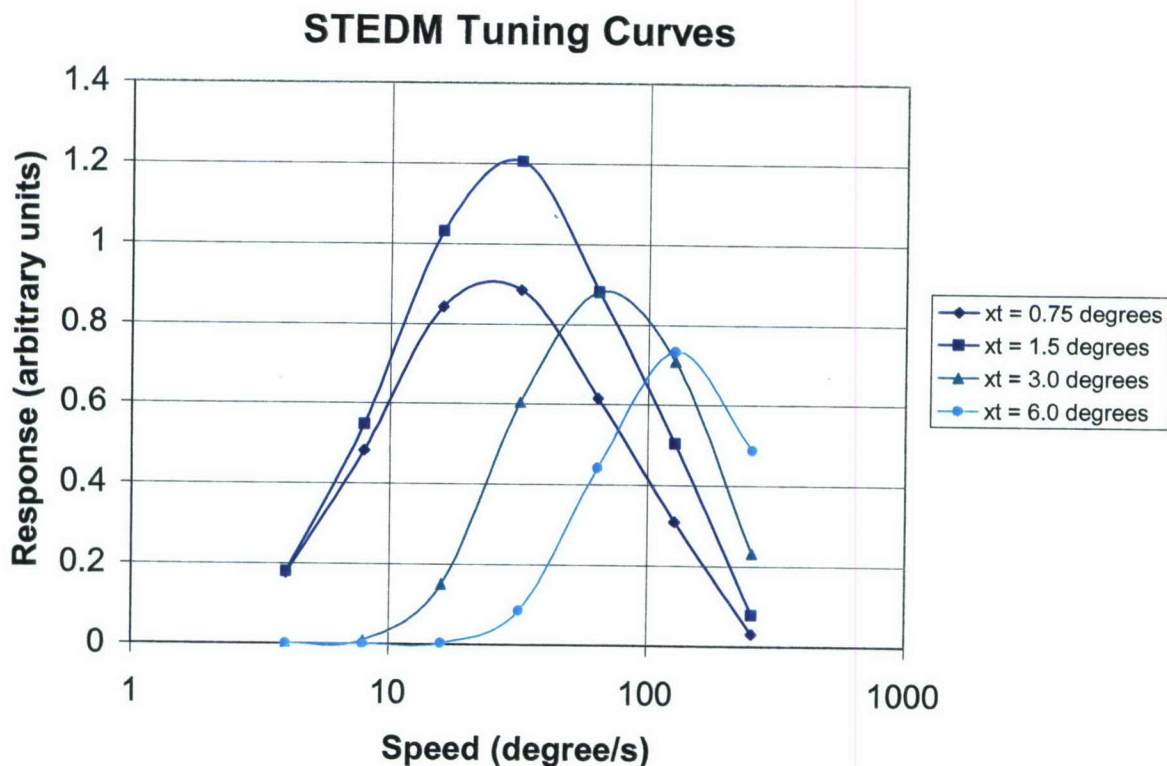


Figure 2: Spatiotemporal tuning curves for the SEMD model. The peak output of the SEMD is displayed as a function of small target speed, with the longitudinal extent of the target, labeled 'xt', as a parameter. Other parameters are the same as in Figure 1.

In the SEMD model there is no delay filtering or other asymmetry applied to either term of the product operation, so the response is not directional (i.e., while it implicitly has an orientation since it is aligned with the axis between two particular ommatidia, it is symmetric with respect to motion in either direction along this axis).

Further Investigations of the SEMD

Following these basic characterizations of the model, we simulated the SEMD in response to the input data in the orbiting target scenarios to obtain further insight into its response to moving background with 'naturalistic' statistics as well as to small targets moving relative to such background. In some of these simulations, as well as by analysis, we investigated the influence of the temporal characteristics of the SEMD temporal highpass filter on the function of the model. The time constant of the filter was varied during these simulations, and in addition, second-order as well as the original first-order filters were evaluated. The conclusions from this phase of the work is summarized as follows.

The fundamental mechanism by which the SEMD operates is the detection of edges (rapid transitions) of opposite slopes at neighboring ommatidia. Thus the filter must be an

edge detector capable of producing opposite-sign responses to leading and trailing edges of a small target, over the range of target speeds (typically tens to one or two hundred degrees per second in the biological system) and sizes (less than one to two or three inter-ommatidial angles) of interest. This means that the filter should reject temporal frequencies including and lower than the fundamental associated with small target passage. The issue can be understood intuitively by considering the response of a first-order highpass filter to a pulse representing transition of a small target across an ommatidium:

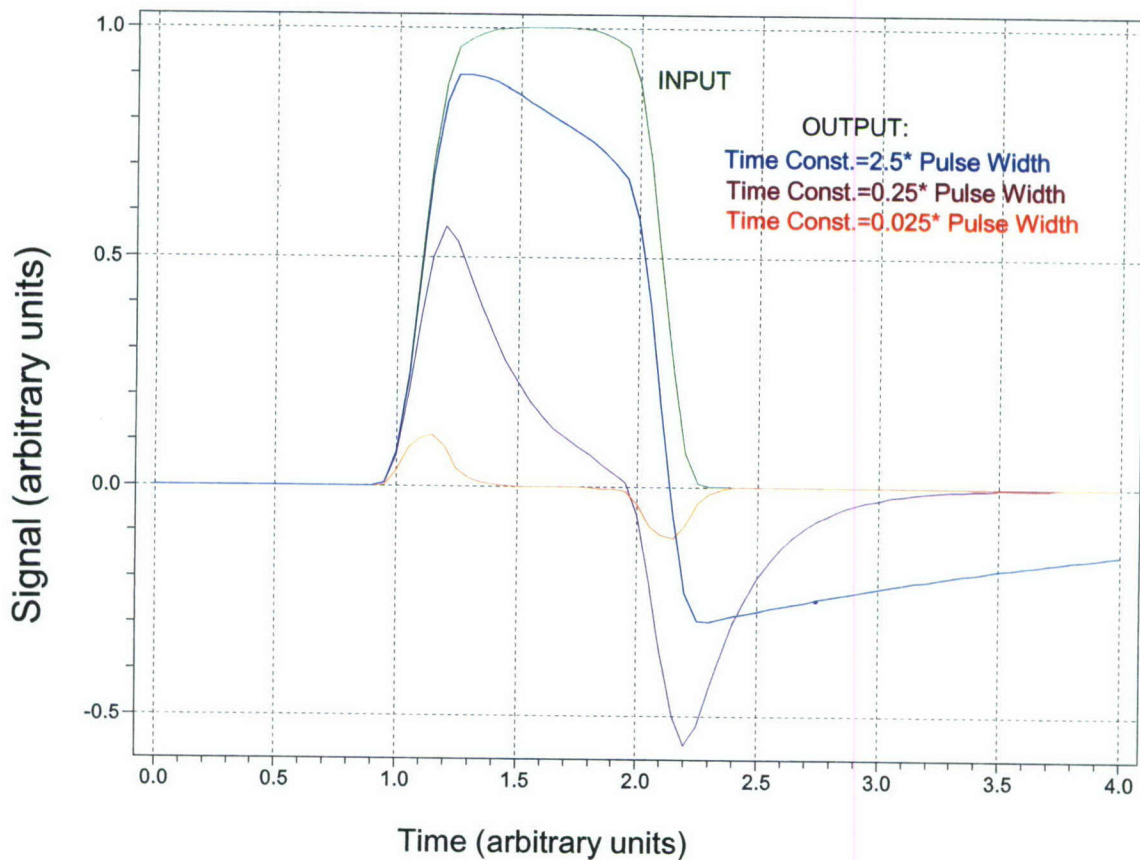


Figure 3: Response of first-order highpass filter to a simulated small moving target input. An input pulse is rounded by blurring due to compound eye optics and early visual processing. The time constant of the filter is a parameter.

When the time constant is long, the filter passes substantial energy of the pulse fundamental and is a poor basis for an edge detector. As the time constant decreases, the filter begins to approximate a differentiator (transfer function $\tau_{ES}/(1+\tau_{ES}) \sim \tau_{ES}$, where τ_E is the highpass time constant) and becomes a better basis for edge detection. As the time constant decreases further, however, the output amplitude falls significantly. Clearly, the time constant must be chosen to give reasonable edge detection over the range of target sizes and speeds of interest, that is, of size $1/\pi$ to $1/(2\pi)$ times the typical event duration in the center of this range. When the background motion behind the target induces relatively large, fast changes in luminance, the time constant needs to be chosen at the lower end of

this range so that the background changes do not prevent the filter from generating two opposite-sign transients in response to target passage. We found that for the orbiting target data, in which the events in early vision outputs associated with target passage were typically of 40ms – 60ms duration, a time constant $\tau_E = 15\text{ms}$ gave good performance in the SEMD. This is shorter than the value arbitrarily chosen during initial characterization (40ms), and results in a larger number of zero crossings for the SEMD filter outputs in response to our input datasets.

In examining the response of the SEMD with a second-order highpass filter, we found that we could obtain larger responses for target relative to background events, than could be obtained with the first-order version. However, the responses of the filter to target edges were generally multimodal, due to the fact that the second-order filter approximates a double differentiator ($\tau_E^2 s^2 / (1 + \tau_E s)^2 \sim \tau_E^2 s^2$) for relevant values of the time constant τ_E . Upon examination, the improvement in target-to-background response was found due to the sharpness of signal transitions with target passage as compared to background motion in our naturalistic input data, and in scenarios (such as urban environments) in which sharp edges are numerous, this advantage would disappear. In addition, the multimodal responses of the filter complicate the detection of small targets by the mechanism of correlation of neighboring responses and rectification for the negative-going phase of the product. Consequently, we selected the first order filter as the standard temporal component for our SEMD model.

Responses obtained for this SEMD model are typically stronger for the target in our data sequences than for background artifacts, even for the small / low-contrast target, in spite of the fact that there is no inherent speed-based discrimination capability in the SEMD. Its responses must therefore be due to the differences between background statistics and the target characteristics, since both are moving at ‘reasonable’ and not too different speeds. Below in Figure 4 is the output of a vertically-oriented SEMD at the ‘3-o’clock’ position on the orbit, where the background and target directions are the same (downward). This is the small / low-contrast target, which transits the SEMD just before 1, 3, and 5 seconds:

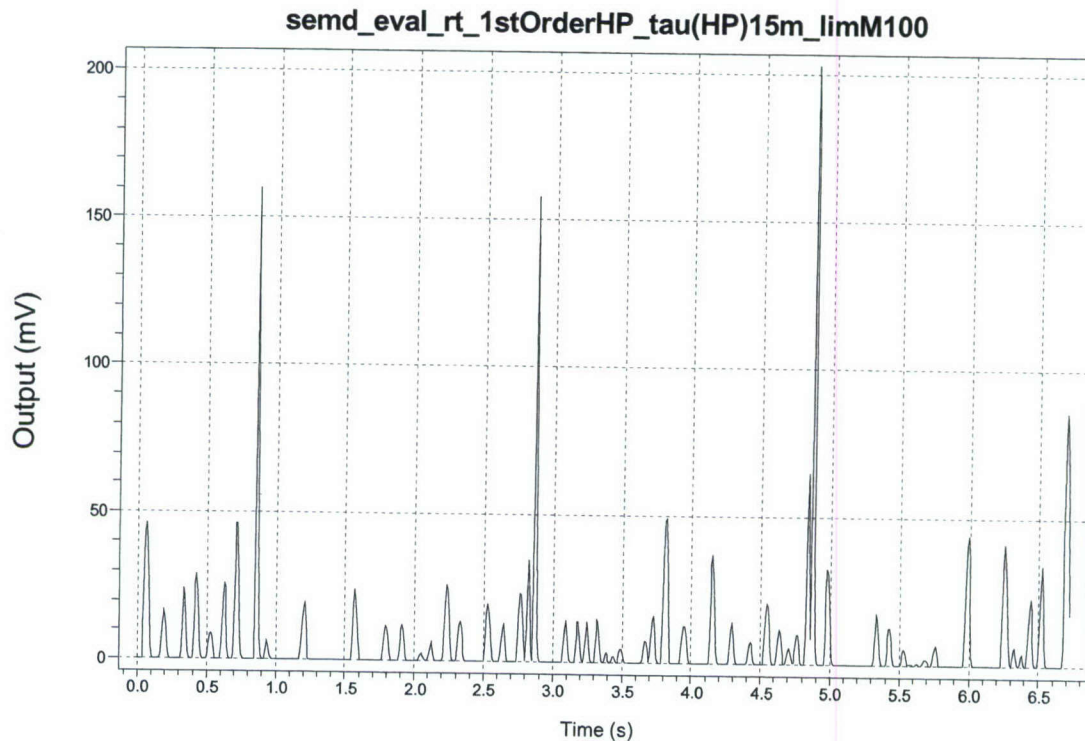


Figure 4: Response of an SEMD to moving input data, with a small target transiting the unit just before times 1s, 3s, and 5s, in the same direction (downward) as background, and with the SEMD axis also vertically oriented. The target is small / low-contrast (scenario 'otslcbds').

Interestingly, the difference between target and background responses is not as pronounced when the target moves in the opposite direction from the background (i.e., at the '9-o'clock' position on the orbit), at least with this particular data sequence. This may be due to 'collision' with opposite-direction events. However, relative velocity would provide a powerful additional discriminant in the case of opposing motion, and target could easily be picked out from background on that basis by subsequent processing.

In the movie segments *semd_array_otlhcbds.avi* and *semd_array_otslcbds.avi* submitted on CD media as supplements to prior progress reports, the response of the standard SEMD model to two of the orbiting target scenarios is shown for full-sized SEMD arrays. These movies use the same color map to indicate intensity as has been used on prior movies for this project. In both video segments, diamond-shaped metapixels are used to display the SEMD outputs, reflecting the fact that there is an SEMD associated with each inter-ommatidial boundary. Each diamond is a tessellation in which the screen pixels are grouped together about the closest midpoint on the boundary between two hexagons, and represents an SEMD that operates on the outputs of early visual processing for the corresponding ommatidia. The orientation of the long axis of each diamond reflects the orientation of the corresponding SEMD. The movie *semd_array_otlhcbds.avi* shows the response to the large/high-contrast target scenario 'otlhcbds', and *semd_array_otslcbds.avi* the response to the small/low-contrast target scenario 'otslcbds'. The response to the small target in *semd_array_otslcbds.avi* is not immediately impressive

to the eye, due to the scintillation of the activated metapixels and the presence of artifacts caused by background. In addition, dropouts occur when the target passes over nearly equiluminant background. Nevertheless, if this video is stepped frame-by-frame, it can be seen that when the target response peaks, it is typically the strongest response found in the entire simulated field of SEMDs. This selectivity is based entirely on small longitudinal size.

In spite of promising results in a variety of simulations, the SEMD was ultimately discounted as a preliminary elementary motion-detecting mechanism in the proposed hierarchy of STMD processing. In experimental work, when biological STMDs are exposed to single traveling edges (the 'extending rod' stimulus), clear responses are obtained when the edge passes through the STMD receptive field (although responses are not as robust as for small objects with both leading and trailing edges). This result is inconsistent with the SEMD because the model depends strictly on the simultaneous passage of a leading edge at one ommatidium with a trailing edge of opposite polarity at a neighbor.

3.1.3. The Primitive Small Target Movement Detector (Shoemaker)

As noted, the PSTMD model is intended to discriminate target from background motion on the basis of relative velocity. The comparison is achieved with an element that is excited by local input, and is also subject to shunting inhibition by a delayed signal passed from a nearby unit. The delayed signal represents an estimate of background motion, with the delay time tuned to reflect the speed of that motion. Background events result in suppression of response by the shunting inhibition, whereas events inconsistent with background motion allow responses to 'break through'.

Further Characterization of the Original PSTMD

Initially, we performed simulations of the PSTMD using the algorithm and arrays developed in the previous effort, but with inputs supplied by SEMDs rather than correlational EMDs or synthetic input signals as used in the prior simulations. We also examined the effectiveness of the PSTMD with shorter-range (nearest-neighbor) anticorrelations rather than the next-nearest-neighbor basis used in prior simulations. Among the conclusions reached were that some degree of smoothing of the SEMD output signals (which as defined above may have discontinuous first temporal derivatives) is desirable when they serve as inputs to the PSTMD, as a means to reduce artifacts in the PSTMD outputs. These artifacts can arise due to the interaction of the sharp changes of an undelayed SEMD signal and the delayed signal which is smoothed by the lowpass filter operation that provides the delay. Some simulations suggested that lowpass filtering of the SEMD output with a first-order filter with relatively short time constant (i.e., 20ms) could improve performance. A second conclusion was that a PSTMD with nearest-neighbor anticorrelations does not allow clear discrimination of target against background at relative speeds that are readily discernible by the human observer. However, even with the longer-range, second-nearest-neighbor interactions, the original model was found to do a generally poor job of distinguishing target from background motion when the velocities are at all similar. As a result we undertook a major revision of the PSTMD model.

Revision of the PSTMD with 'Propagating Predictors'

This revision was the primary accomplishment on the present project with respect to the PSTMD. It constitutes an elaboration of the original model in which the signal estimating background motion was generated as a *propagating predictor* with spatial as well as temporal memory. A schematic diagram illustrating the propagating predictor concept is given below in Figure 5:

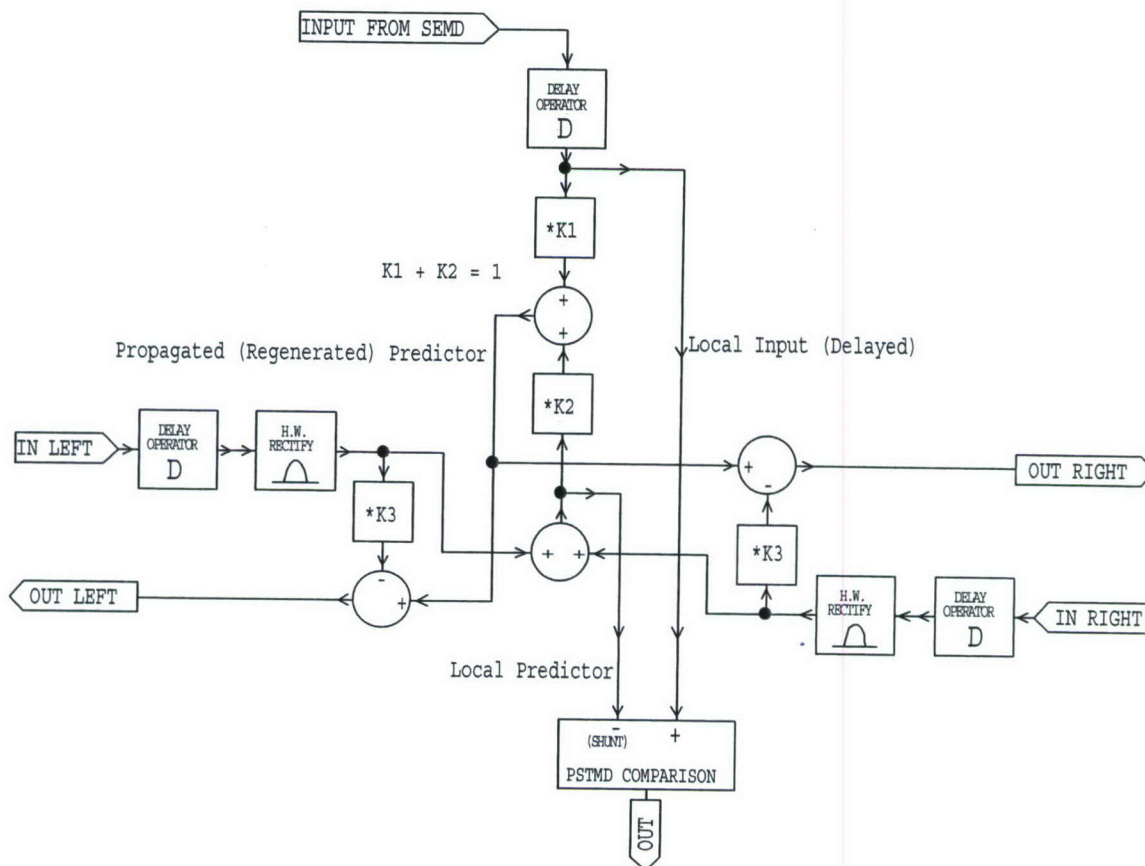


Figure 5: 'Propagating predictor' for background motion in a PSTMD model. This example is for a unit in a uniaxial or one-dimensional array.

This diagram depicts one element of a one-dimensional or uniaxial network, with a pair of connections to units to the left and to the right, and with a local input presumed to come from an SEMD. The delay operator is applied to the both the local input (*INPUT FROM SEMD*) and lateral predictor inputs (*IN LEFT* and *IN RIGHT*). The comparison of the predictor signal to the input signal takes place after application of the delay, so that the shape (harmonic content) of the input signal is similar to that of the predictor in response to a moving event. Local (additive) inhibition occurs on the reciprocal connections (*OUT LEFT* and *OUT RIGHT*) that propagate the predictor signal from the element to its neighbors, so that when an event is initially propagated from a neighbor into the element, subsequent propagation from the element back to that neighbor is inhibited. In this way, predictor propagation is unidirectional for unidirectional motion. The only nonlinearity in

the predictor network is the half-wave rectification that occurs on each lateral input. The comparison operation between the predictor and (delayed) input signal computed by this network takes place by the same shunting inhibitory mechanism used in previous PSTMD versions, that is to say, division by the predictor signal summed with a small constant to prevent singularity. Tuning of the delay operator to the speed of background motion was done by hand in simulations; approaches to automatic feedback tuning were considered but not developed beyond the conceptual stage.

Following initial simulations, we spent some time analyzing the delay operator used in the PSTMD model in the context of its input signals, which are assumed to come from SEMDs. The SEMD produces only positive pulses due to the nature of its processing, and furthermore, the desired delay time of events in SEMD output space tends to go as the duration of such events, since they represent stimuli in which a leading increase in luminance correlates with a trailing decrease, or vice-versa, and such events are moving continuously across pairs of ommatidia. One conclusion regarding the PSTMD delay is based on the straightforward observation that the phase delay induced by a linear lowpass filter increases with its order, while for a given phase delay, the attenuation and change in harmonic content of the output relative to the input signal decrease with increasing order. Thus a high-order filter with a relatively short time constant is desirable to implement the delay operator. The second conclusion is that it is desirable to implement the filter with complex poles, which improve the transient response time and decrease attenuation relative to real poles, in the neighborhood of the corner frequency. We achieved promising results with a filter order of six (i.e., three complex pole-pairs) and with a quality factor Q of 0.65-0.7 (with $Q=0.5$ defining the limiting case of real poles). Results improve if the order is increased beyond six, but with decreasing returns for the increased computational complexity (and circuit complexity if an analog VLSI model were to be fabricated).

Below in Figure 6 are shown the results for a one-dimensional predictor network in response to data taken from the scenario 'otslcbds':

mentioned in Section 2.1.6), but ultimately, poor predictor performance due to spurious propagation could not be overcome, and as of the project's end no two-dimensional generalization of the PSTMD had been found allowing relative velocity-based target discrimination remotely approaching that of the one-dimensional model.

3.1.4. *The Elementary Small Target Motion Detector (Shoemaker, O'Carroll)*

As noted, our ESTMD models have been based on the observed characteristics of the class of neurons that we have also labeled ESTMDs. The basic operation of our model depends on a receptive field in retinotopic space with a notched inhibitory surround and an excitatory center, and 'tonic' or persistent responses in each region. This is implemented with the following functional elements:

1. A nonlinear (fast onset / slow decay) temporal element. This displays a persistent response following an input stimulus.
2. A diffusive network for passive electrotonic spread of inhibition. This network receives inputs from a nonlinear temporal element.
3. A summing neuron that forms a receptive field with excitatory center and a notched inhibitory surround, by virtue of the pattern of interconnection weights with excitatory temporal elements and with the inhibitory network.

In the intended mode of operation, only when a target enters the receptive field via the notch, and is small enough laterally to fit through the notch, can the summing neuron reach a net state of excitation. If a target enters by any other direction, the persistent inhibition that it recruits is supposed to be sufficient to preclude a net excitatory response when it reaches the excitatory region.

The ESTMD Temporal Element and the 'Sustained Tonic' Response

Initial work during the present contract focused on the 'persistent' temporal element. Near the close of the prior contract, we demonstrated the operation of the nonlinear or 'tonic' temporal filter in the silicon ESTMD in an 'overdriven' mode. In this mode, following any transient input excitation that exceeds some threshold level, the temporal element remains fully active for a length of time (determined by the bias of the filter circuit) before it decays. This is a favorable characteristic for purposes of modeling the ESTMD neuron, allowing more robust responsiveness (i.e., adequate function over a wider range of target characteristics and speeds). The 'tonic' operation of the nonlinear circuit previously constituted a slow constant decay of post excitation response, rather than any period of sustained response. We developed a mathematical behavioral model for the 'sustained tonic' mode, with the characteristics (i.e., period of activity and decay time) controllable in a flexible manner by a relatively few parameters. This additional flexibility could be readily extended to the circuit with some simple modifications. The series of operations can be summarized as a clipping or squashing nonlinearity applied to the input, followed by a fast-onset, slow-decay nonlinear filter, followed by a second clipping operation, at a lower signal amplitude than the first. The governing differential equations are given in (3):

$$\begin{aligned}
 x &= \text{input}; z = \text{output}; \\
 y_1 &= 1/2(\tanh[g \cdot (x - a)] + 1)
 \end{aligned}
 \tag{3}$$

$$\dot{y}_2 = (\exp[b(y_1 - y_2)] - 1) / \tau$$

$$z = c \cdot \tanh[y_2 / c]$$

where g , a , b , and c are constants with g and a chosen based on the input signal characteristics, $c < 1$, and where τ is a time constant corresponding to persistence time of the nonlinear filter. The y_1 and y_2 are intermediate variables introduced for clarity, and a dot over a variable indicates time derivative.

The response of this model to a transient input is illustrated below in Figure 6:

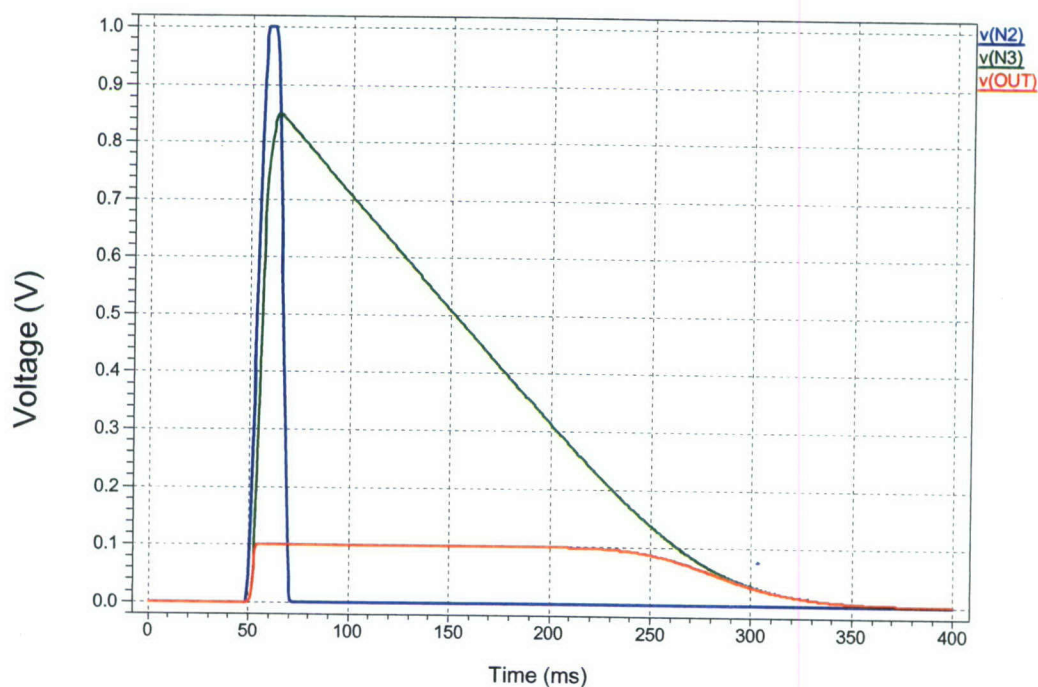


Figure 7: Response of the 'sustained tonic' temporal element. The blue trace is the input to the nonlinear filter, the green trace is the output of the filter, and the red trace is the final output.

Further Development of the SEMD Model

Following development of the 'sustained tonic' temporal model, we made several additional changes to the ESTMD algorithm and topology relative to the previous effort, prior to further simulations. First, we supplied inputs to the ESTMD from SEMDs rather than from earlier visual stages. (PSTMDs were not included due to lack of success in formulating two-dimensional architectures.) Rather than the single temporal element used in prior work, we began to use two elements with different persistence times for the excitatory and inhibitory signals, with the inhibitory unit assigned a longer time constant than the excitatory unit. One such pair of units is included for each SEMD, both receiving input from the SEMD. Finally, the receptive field size of the model ESTMD was expanded, to make it closer to those of biological ESTMDs (previous models had a single-pixel excitatory center). The revised model included a diffusive inhibitory network, and the

pooling of excitatory and inhibitory inputs was modeled with a linear weighted sum, as in previous models.

In this new architecture, connections are made from these elements onto an ESTMD 'neuron' without regard to the orientations of the underlying SEMDs, i.e., orientation selectivity is not maintained by choice of SEMDs which feed an ESTMD neuron. Rather, orientation selectivity is regained – and direction selectivity established – by the *spatial pattern* of inter-connections from the inhibitory and excitatory elements onto the ESTMD neuron. The particular pattern of connectivity that we used is illustrated below in Figure 8:

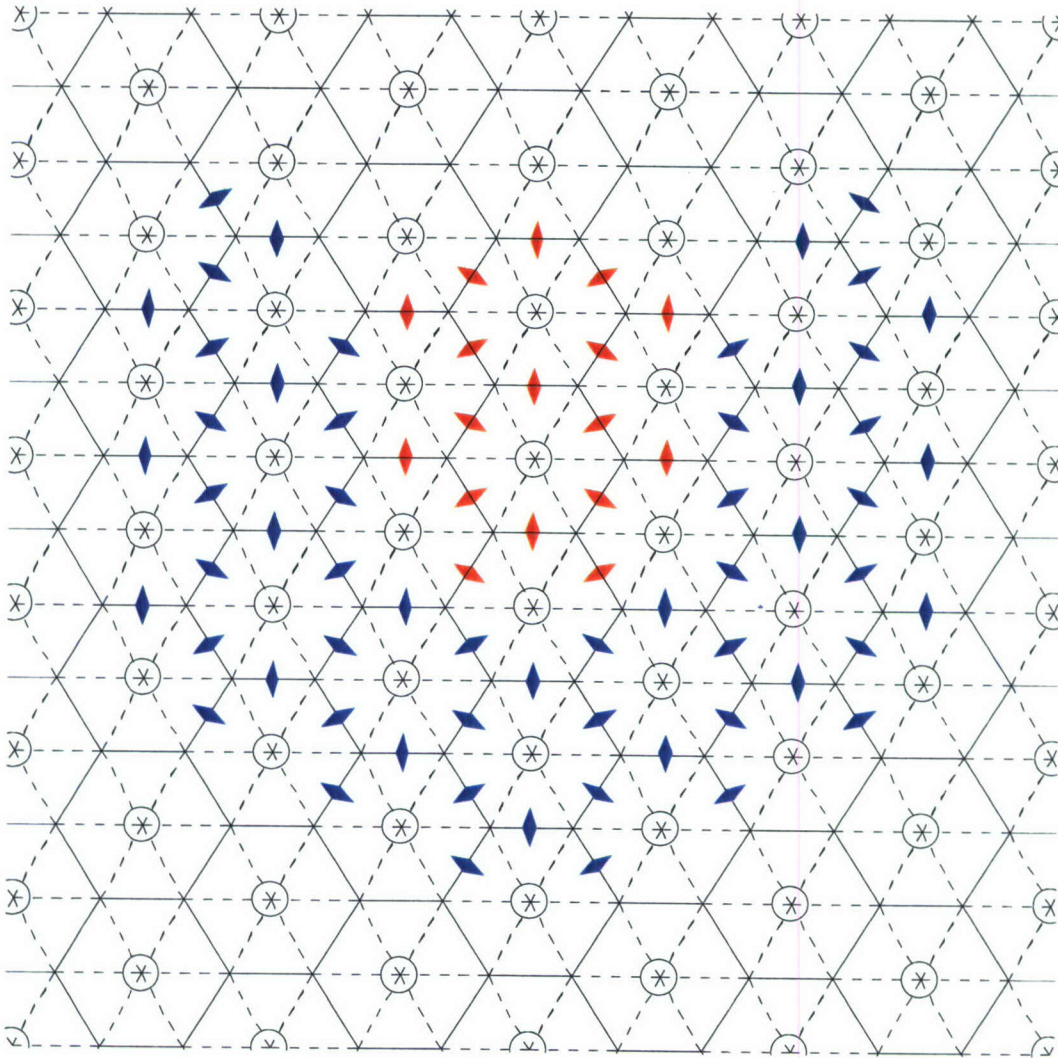


Figure 8: Depiction of interconnection pattern which establishes the receptive field of a model ESTMD neuron in retinotopic space. Hexagons with solid boundaries indicate ommatidia, and tetrahedrons (diamonds) with dashed boundaries can be regarded as indicating SEMDs as well as elements in the inhibitory and excitatory networks that operate temporally and spatially on SEMD outputs. A red mark at the center of a tetrahedron indicates a connection from the corresponding excitatory element onto the ESTMD neuron proper, and a blue mark indicates a connection from the corresponding inhibitory element onto the ESTMD neuron.

This pattern gives the ESTMD an excitatory receptive field area of about three degrees extent (i.e., it should begin to reject moving stimuli when they are significantly larger than 3° in lateral size), inside a notched inhibitory receptive field area. In our simulated arrays, these model ESTMD neurons are arranged in a hexagonal grid in retinotopic space, at twice the pitch of individual ommatidia. It is assumed that a complete system would have one set of such ESTMDs aligned with each of the six principal directions of the hexagonal grid. However, we generally simulated ESTMDs with a single preferred direction, and varied the direction of motion of visual objects in order to investigate directional selectivity.

Initial simulations with the revised ESTMD model were aimed at developing a grasp of the response characteristics versus expectations, and also at tuning of ESTMD parameters. The first step in ESTMD processing, represented by the first of Eqns. (3), provides signal limiting but also a 'soft thresholding' function by virtue of subtraction of the threshold parameter a in the argument of the \tanh . Because target events typically (but not always) cause larger responses in the SEMD outputs than background events in our sequences, we attempted to set a and the gain g such that most artifacts were suppressed while target events resulted in saturation. In the nonlinear 'sustained tonic' filter represented by the second and third of Eqns. (3) the parameter b was set with to 10 for rapid activation, and the persistence time τ was set to 100ms for the excitatory element and 250ms for the inhibitory element, to insure that inhibition is able to prevent net excitation of the ESTMD neurons when a target passes through the receptive field in the antipreferred direction. In addition, the shunt and lateral conductances in the electrotonic inhibitory network were set to equal values, resulting in a relatively small space constant (on the order of one unit)

Following these initial simulations, we attempted for the first time the simulation of complete ESTMD arrays with early vision and SEMDs as precursor processing. Results were moderately encouraging. We did expect and observed a significant number of artifacts in the outputs due to the fact that our input data contains both target and background motion, and the precursor processing – the SEMD – has no relative velocity-based discrimination capability and does respond to the motion of small background features as well as targets. In addition to these expected artifacts, we also observed poorer-than-expected rejection of larger background features.

In these simulations, the receptive fields in the model ESTMD neurons were formed with the arbitrary choice of unity weights for all excitatory connections depicted in Figure 8, and weights of -1.5 for the inhibitory connections. We performed a limited number of simulations in which these parameters and the nonlinear filter parameters were varied, but did not do any systematic optimization of the model.

3.1.5. Rectifying Transient Cells (Shoemaker, Wiederman)

The class of rectifying transient neurons includes neurons that in the past have been recorded from the first optic chiasm, representing the axons of afferent neurons projecting from lamina to medulla (in fly, Jansonius and van Hateren, 1991, 1993a), and from cells in or projections into the medulla (in locust, Osorio, 1987, 1991). Recordings from blowflies in the O'Carroll laboratory appear to be from intrinsic medulla neurons, although it is possible they may be from cells projecting to or through the medulla from elsewhere (i.e., from laminar RTCs).

The published and observed characteristics of RTCs, and our experiences in modeling them, have given us for the first time (at least tentatively) a putative precursor element on which to build more elaborated, and we hope better-performing, STMD models.

Initial Model for the RTC

Based primarily upon previously published data on RTCs, we developed an initial computational model that is consistent with the spatial and temporal characteristics of the lamina RTC (the so-called ‘on-off’ cell). This model is illustrated below in schematic form in Figure 9:

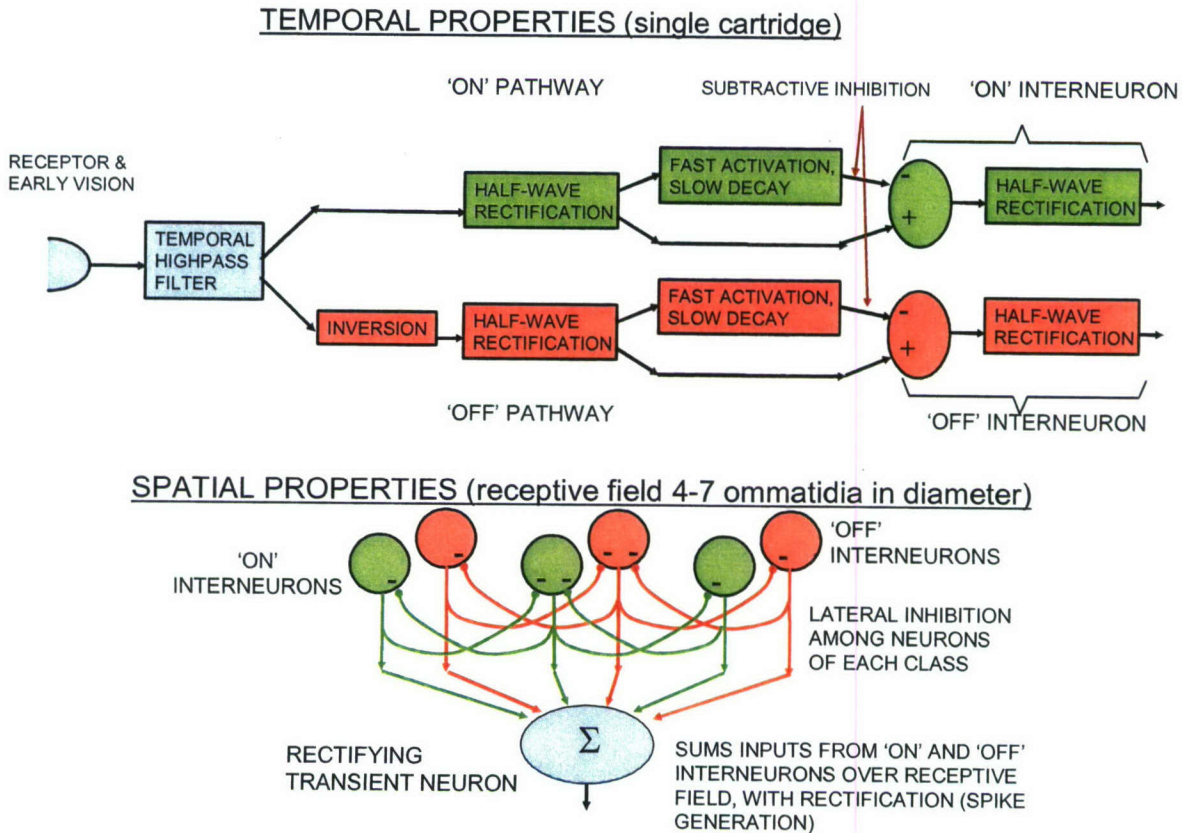


Figure 9: Block diagram depicting a model for the processing associated with a rectifying transient neuron, analogous to the lamina ‘on-off’ cell. At top are elements associated with a single optical cartridge up to the level of individual ‘ON’ and ‘OFF’ neurons, which illustrates the origins of the temporal characteristics of the cell. At bottom is shown the interaction between and summation of signals from ‘ON’ and ‘OFF’ elements in multiple adjacent cartridges, which give rise to the spatial characteristics of the receptive field.

In this model, the signal path leading to the rectifying transient cell is divided into distinct ‘ON’ and ‘OFF’ channels at a relatively early stage. In this regard, it is similar to a detailed model for the lamina on-off cell (Sarakaya, Wang, and Ögmen, 1998) but differs from other prior models for RTCs (Jansonius and van Hateren, 1993; Osorio, 1991), which have placed rectification later in the processing. This assumption predicts the existence of two populations of lamina neurons to carry the ON and OFF signals; Sarakaya et al. (1998)

suggest that these may be two distinct types of lamina amacrine cells, but we note that the lamina monopolar cells (LMCs) and the ‘sustaining’ neurons (tentatively associated with lamina L5 cells, Jansonius and van Hateren (1993)) have transient and opposite-polarity responses to luminance changes, and could thus be part of the two pathways.

In our models, the input to both ON and OFF channels is assumed to be strongly highpass-filtered in the temporal domain and inverted in one case, then half-wave rectified. The signals in the two channels are thus transient and of the same polarity, although they reflect opposite phases of the input waveform. Adaptation in each channel is achieved by means of subtractive inhibition. The input signal is processed by an element (presently assumed to be a distinct interneuron) with fast activation and slower response decay, with an output corresponding to a ‘state of adaptation’ for that channel. This output is subtracted from the original signal and then half-wave rectified by a subsequent interneuron, so that only signal levels above the ‘state of adaptation’ are passed on. Corresponding to this second interneuron are the ‘ON’ and ‘OFF’ interneurons in the top part of Figure 9.

The spatial characteristics of the rectifying transient cell are modeled by assuming that ‘ON’ and ‘OFF’ interneuron outputs are summed over a number of neighboring cartridges. Prior to this stage, however, lateral inhibition takes place between interneurons of each class, leading to reduction of response when an increasing number of cartridges are stimulated with luminance changes of the same polarity, as observed by Jansonius and van Hateren (1993a). The receptive field of the ‘on-off’ cell is reported by Jansonius and van Hateren (1993a) to have a spatial extent of 4 – 7 ommatidia.

An initial version of this model for simulation purposes was built from abstract elements in the SPICE environment. The highpass filter at top in Figure 9 is composed of linear elements, and sums and differences are likewise linear operations in the usual sense. Signal rectification is ideal half-wave rectification ($\text{POS}(x) = (|x|+x)/2$). The ‘fast activation, slow decay’ characteristic used to compute the ‘state of adaptation’ for an ON or OFF channel is modeled with a nonlinear (diode) conductance charging a capacitance, which then discharges through a linear resistance.

Modeling the RTC with ‘Neural Primitives’

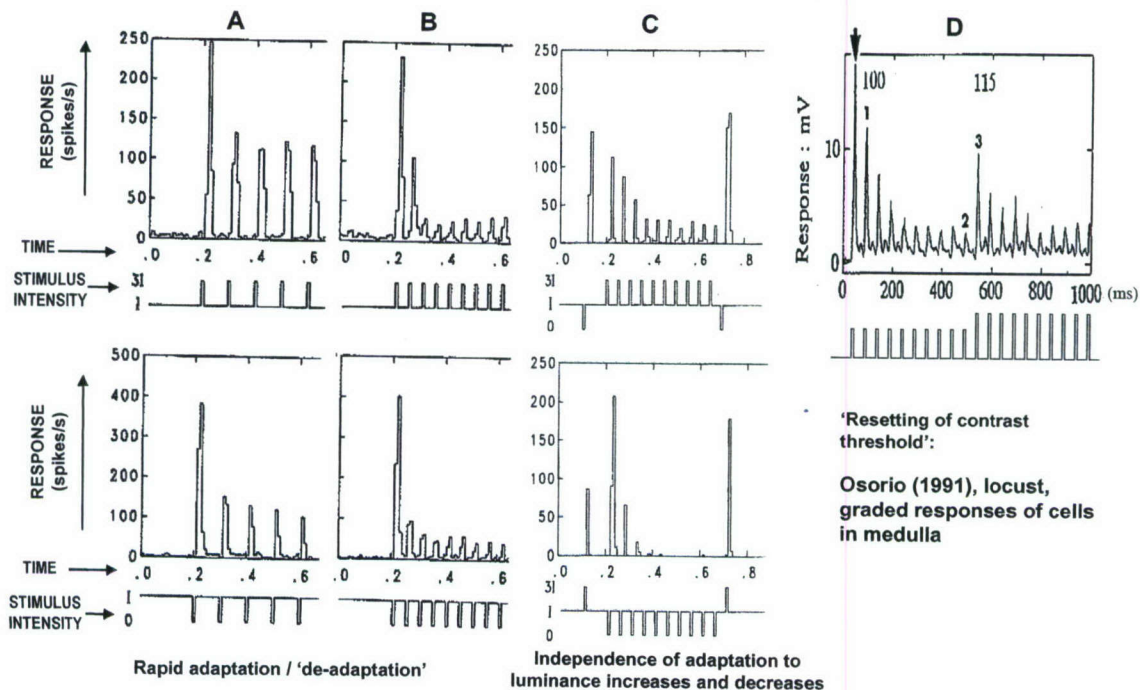
In later versions, some of these functions were modeled in a way that makes them more consistent with actual neuron biophysics. Interconnections between neuronal analogs are made with ‘chemical synapses’ that comprise a variable conductance in series with a voltage source representing an ionic reversal potential. Summation of excitatory and inhibitory synaptic currents implements ‘sums’ and ‘differences’ (which do not have the usual linear sense because synaptic currents are non-linearly related to the input signals). The ‘fast activation, slow decay’ characteristic is achieved naturally with an interneuron model that has a large membrane time constant, and input synapses whose modulated conductances are considerably larger than the intrinsic membrane conductance for typical inputs. In some simulations, a multi-compartment neuron is used with a ‘dendritic’ cable interposed between the synapses and output site (‘cell body’). Finally, the half-wave rectification is replaced in some cases by a smooth bounded strictly-positive function (i.e., a sigmoid whose range is positive), meant to represent transformation between membrane potential and ‘output’ (either firing rate, or neurotransmitter release at a target cell).

This work was done in the SPICE environment that has been used for simulations to date by the industrial partner. One aim of developing more biophysically realistic

processing primitives than in past versions was to initiate work on a general 'neural toolkit' in the SPICE environment that could eventually be useful (and supplied to other interested modelers with electronics backgrounds) for multi-compartment neural modeling of the kind that is now performed with tools such as GENESIS and NEURON. Although such a 'toolkit' is far from complete at this stage, an initial collection of useful modules has been developed.

Simulation Results for RTC Temporal Characteristics

Initial simulations focused primarily on the temporal characteristics of the RTC. To give a qualitative idea of the capabilities of the model, below we compare some preliminary results (Figure 11) from the more biologically-faithful version of the model to results obtained by Jansonius and van Hateren (1991) and Osorio (1991) in electrophysiological experiments testing the temporal properties of RTCs (Figure 10).



Jansonius and van Hateren (1991), blowfly, axons of spiking cells in first optic chiasm (lamina→medulla)

Figure 10: Prior electrophysiological results for rectifying transient cells. Parts *A* – *C* are for blowfly lamina on-off cells, and *D* for an RTC recorded from locust medulla. Parts *A* and *B* show rapid, frequency-dependent adaptation to luminance pulses, corresponding to both increases (top) and decreases (bottom) in intensity from a reference level *I*. The full-wave-rectifying nature of the response is clear. Part *C* illustrates independence of adaptation to increases and decreases in luminance. Part *D* shows how increasing the intensity of a periodic pulse stimulus causes a 'breakthrough' of the response from adapted levels, or alternatively, a 'resetting of the contrast threshold' (Osorio, 1991).

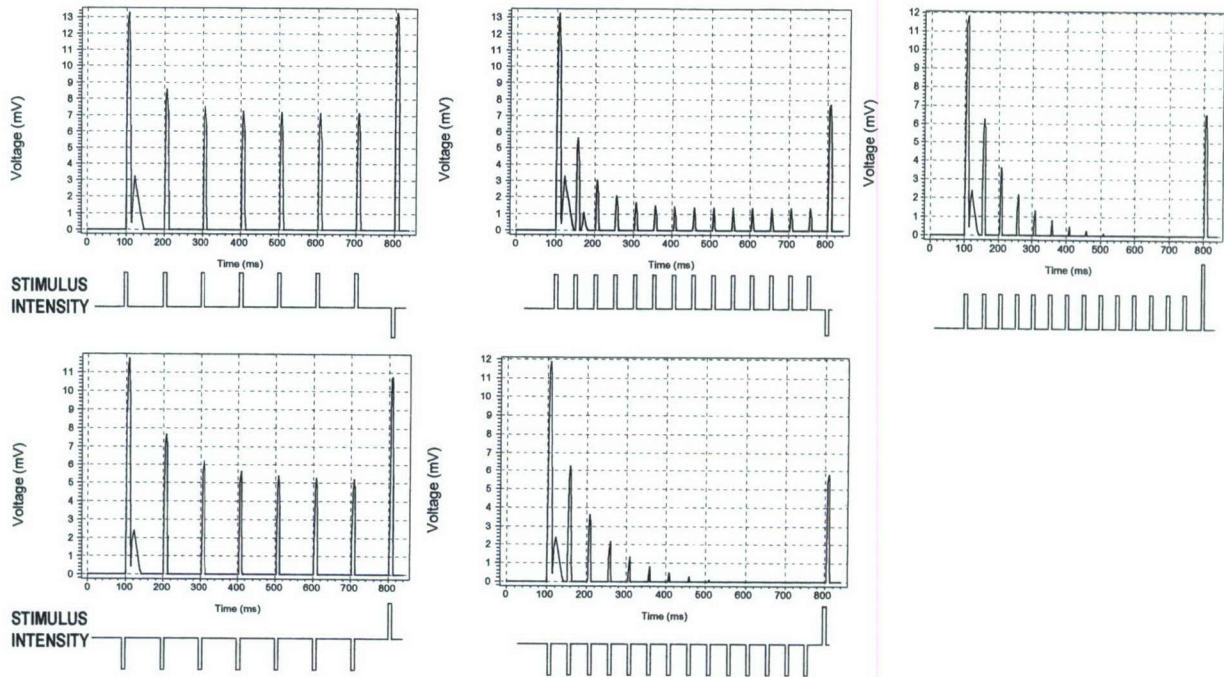


Figure 11: Simulated responses for rectifying transient cells. The four panels at left may be compared with electrophysiological results *A*, *B*, and *C* in Figure 10. The right-most panel may be compared with part *D* in that figure.

3.1.6. NMDA Receptors and Bistable / Amplifying Neural Behavior (Shoemaker)

Perhaps the most significant conclusion of the study of NMDA receptors is that bistability mediated by these receptors requires the presence of additional membrane conductance, and that there is an upper bound on the equivalent reversal potential associated with that additional conductance. Using the Jahr-Stevens (1991) model for NMDA conductance and under physiological values of extracellular $[Mg^{2+}]$, this maximum reversal potential value is found to be about $-78mV$. This implies that substantial potassium conductance must be present to enable bistability. The only major synaptically-mediated ion channel whose primary permeability is to potassium is the $GABA_B$ receptor, and so much of the analysis considered the effects of coactivation of NMDA and $GABA_B$ synapses. In addition to a maximum condition on the equivalent reversal potential, limits (corresponding to fold bifurcations) were computed on the ratio of NMDA to total ohmic conductance compatible with bistability. Outside of bistable regimes, amplifying effects of NMDA receptors were noted, and maximum gains demonstrated to occur again with co-occurrence of strongly depolarizing (i.e., potassium) currents. Dendrites terminating on a somatic load resistance were analyzed numerically, and bifurcation between mono- and bistable regimes shown to occur as the electrical length of the dendrite is varied, in addition to bifurcations with variations in NMDA and depolarizing conductances in the membrane. Finally, fast AMPA and $GABA_B$ inputs were shown capable of triggering transitions between stable states when a compartment or dendrite is in a bistable regime.

A manuscript detailing the results of the study was prepared and submitted to PLoS Computational Biology, but was rejected. It is presently in revision and will be resubmitted to another journal near or shortly after termination of the grant.

3.1.7. Silicon Modeling (Shoemaker)

On the DARPA / MIT/Lincoln Labs 3DM2 run, Tanner Research reserved and utilized space corresponding to two Mosis 'tiny chips' (2mm square each), each with three interconnected vertical tiers. One of these 3-D chips contains a silicon model for an RTC, and the second a model for a correlational EMD. The parts of these models are distributed among the tiers as follows. The first tier of each stacked chip contains a photodetector (with design guidance provided by E. Culurciello at Yale University), an exponential (subthreshold MOS) load for the photocurrents to provide logarithmic compression, and a first-order lowpass G_m -C filter as an initial stage for subsequent temporal operations. The second tier circuits are also common to both chips, and include a differential circuit to compute a highpass output as the difference between the first-tier raw and lowpass-filtered signals, two circuits for half-wave rectification of each waveform phase, a nonlinear filter (fast rise, 'sustained tonic' response) for each of these separate ON and OFF channels, and a shunting inhibition / gain control stage to model adaptation. For the RTC model, the third tier contains circuits to perform spatial inhibition, and to recombine the ON and OFF channels. For the EMD model, the third tier contains circuits to perform a delay (lowpass filtering) operation, a one-quadrant log-domain correlation, and to recombine signals differentially to obtain a bipolar output. This EMD model is novel in employing the RTC model for nonlinear adaptation as a model for motion adaptation. Schematic diagrams of the circuits are depicted below in Figure 12 - Figure 15.

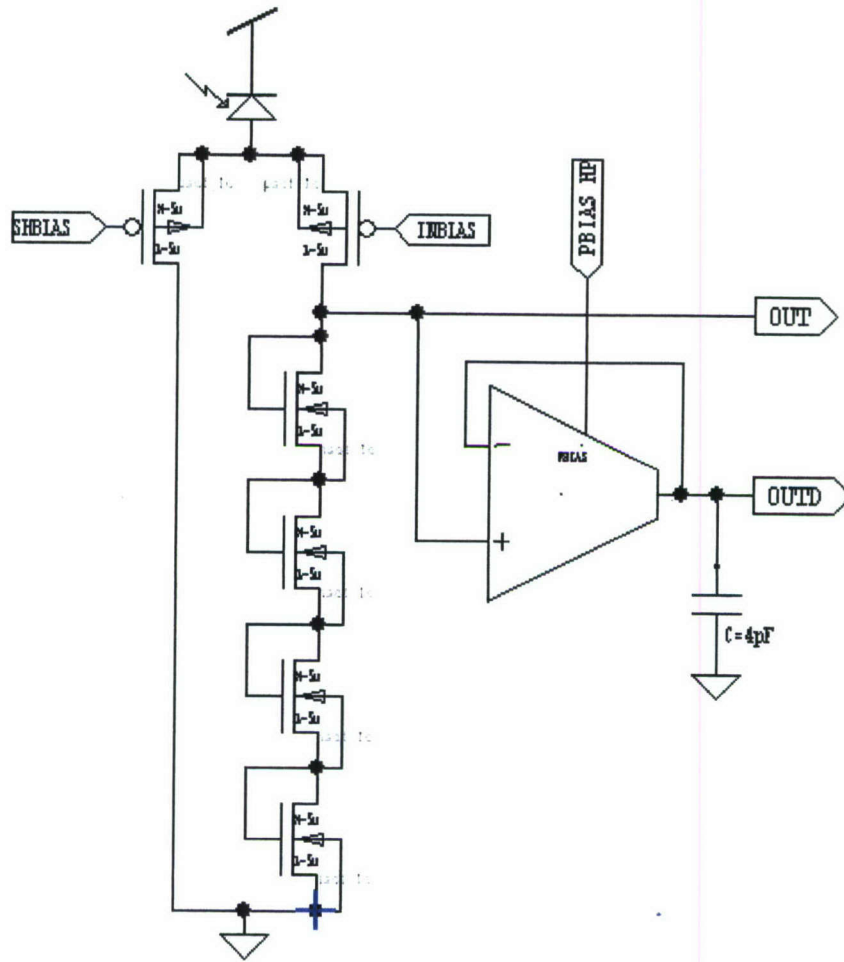


Figure 12: First-tier circuits, including photodiode, exponential load, and G_m -C filter, for 3-D RTC and EMD silicon models.

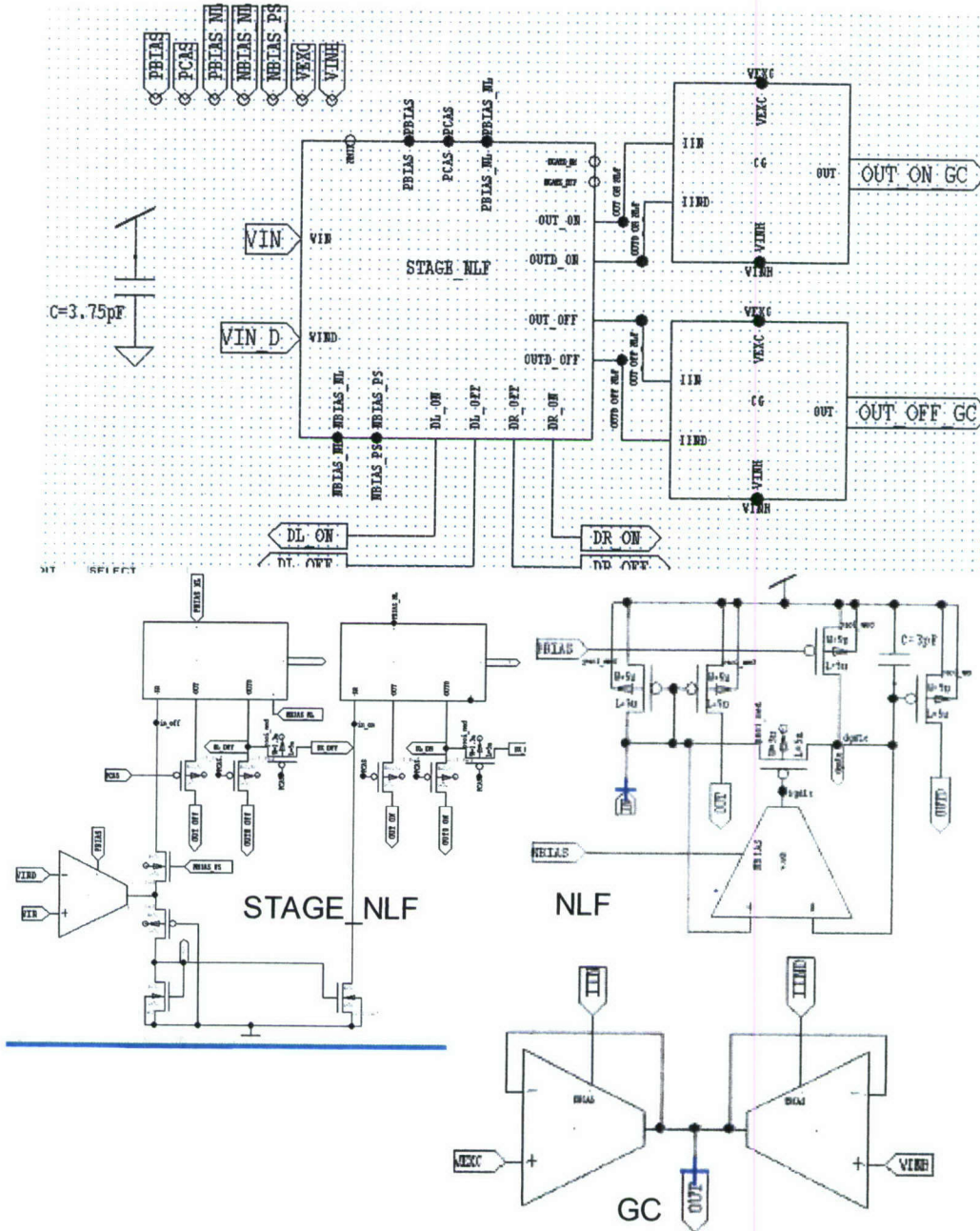


Figure 13: Second-tier circuits, including ‘sustained tonic’ filter and adjustable gain circuits, for 3-D RTC and EMD silicon models.

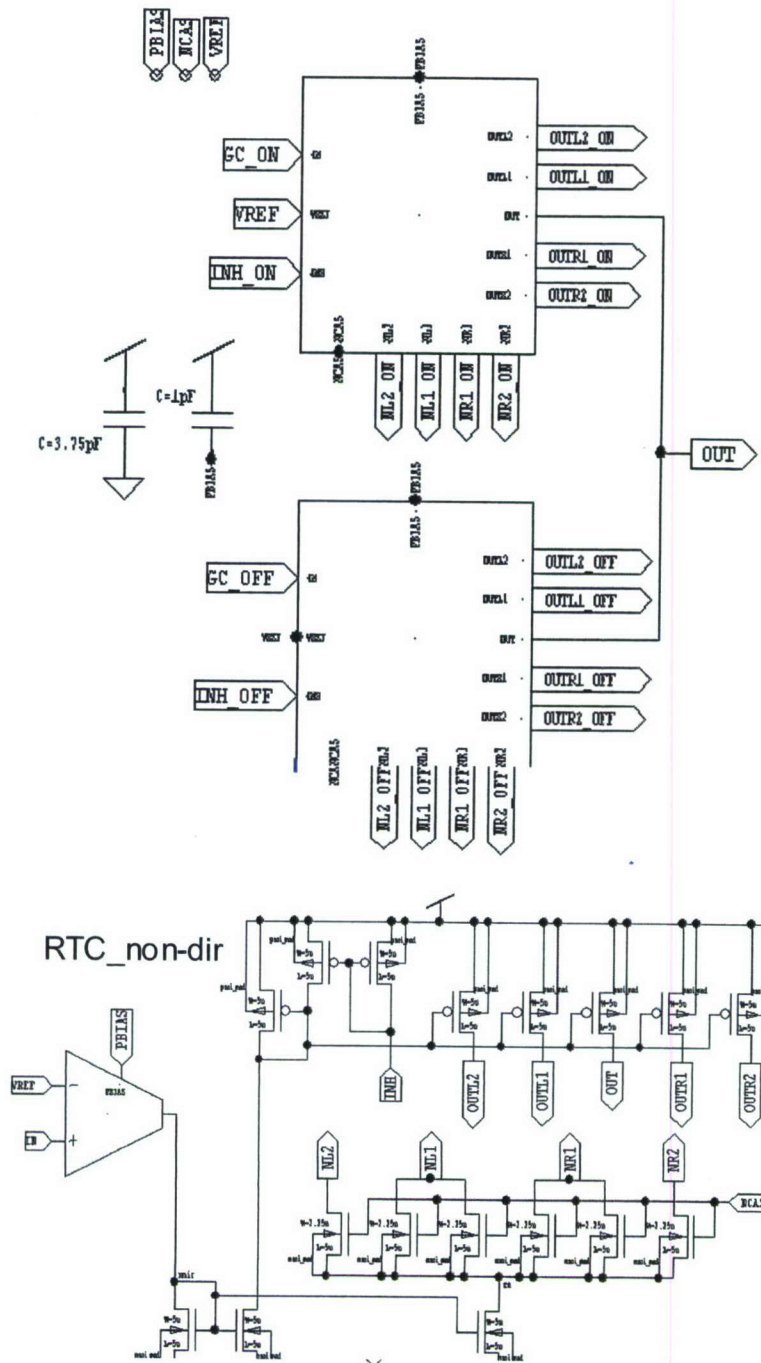


Figure 14: Third-tier circuits for 3-D RTC model.

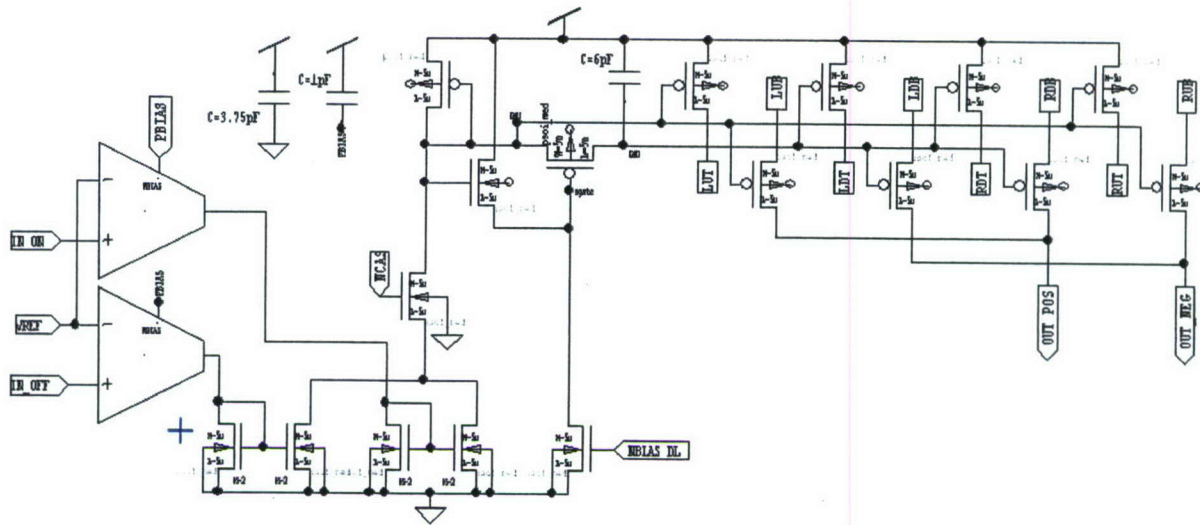


Figure 15: Third-tier circuits for 3-D EMD model.

A single submission of two test die containing bio-inspired circuits was made to a DARPA-sponsored fabrication run of an experimental three-dimensional (three interconnected interconnected wafer tiers) integrated circuit process. The period of performance of the grant was extended to permit receipt and testing of these circuits, but unfortunately delays in the completion of this fabrication have precluded test and evaluation.

4. Personnel Supported

Patrick Shoemaker, Tanner Research, Inc., Co-Principal Investigator
 Thomas Bartolac, Tanner Research, Inc., Senior Scientist
 David O'Carroll, University of Adelaide, Co-Principal Investigator
 Karin Nordström, University of Adelaide, Post-Doctoral Fellow
 Steven Wiederman, University of Adelaide, PhD Student
 Paul Barnett, University of Adelaide, PhD Student
 Douglas Bolzon, University of Adelaide, PhD Student
 Bart Geurten, Diploma (exchange) student from University of Köln, Germany
 Russell Brinkworth, University of Adelaide, Post-Doctoral Fellow
 Lachlan Dowd, University of Adelaide, Computer Support Officer

5. Publications

5.1. Papers Produced Under Support of this Grant:

Shoemaker, P. A methodology for long time-constant log-domain filters in CMOS. *Analog Integrated Circuits and Signal Processing*, Vol. 42, pp. 161-178, 2005. (Produced under prior contract but appearing in print during the term of this grant.)

Nordström, K., and O'Carroll, D.C. Insect detection of small targets moving in visual clutter. *PLoS Biology* vol. 4 (3), pp. 378-386, 2006. DOI: 10.1371/journal.pbio.0040054

Nordström, K., and O'Carroll, D.C. Small target detection neurons in female hoverflies. *Proceedings of the Royal Society of London B*, vol. 273 (1591), pp. 1211-1216, 2006. DOI: rspb.2005.3424

O'Carroll, D.C., Barnett, P.D., Mah, E.L. Nordström, K and Brinkworth, R.S.A. A neuromorphic model for a robust, adaptive photoreceptor reduces variability in correlation based motion detectors. *BICS 06, Brain Inspired Cognitive Systems*, 2006.

Barnett, P.D., Nordström, K and O'Carroll, D.C., Retinotopic Organization of Small-Field Target Detecting Neurons in the Insect Visual System. *Current Biology*, Vol. 17, pp. 569-578, 2007.

Guerten, B.R.H., Nordström, K., Sprayberry, J.D.H., Bolzon, D., and O'Carroll, D.C., Neural mechanisms underlying target detection in a dragonfly centrifugal neuron. *Journal of Experimental Biology* vol. 210, pp. 3277-3284, 2007.

Shoemaker, P.A. Analysis of neural bistability and amplification mediated by NMDA receptors. In preparation/revision, 2007.

5.2. Papers by the Principals in Related Areas

Shoemaker, P.A., O'Carroll, D.C., and Straw, A.D. (2005) Velocity constancy and models for wide-field motion detection in insects. *Biological Cybernetics*, Vol. 93, No. 4, pp. 275-287, 2005.

Guzinski, R., Nguyen, K., Yong, Z.H., Rajesh, S., O'Carroll, D.C., and Abbott, D. Characterization of insect vision based collision avoidance models using a video camera. *Proceedings SPIE* Vol. 6036, pp. 328-342, 2006.

Rajesh, S., Abbott, D., and O'Carroll, D.C. A 16 pixel yaw sensor for velocity estimation. *Proceedings SPIE* vol. 6036, pp. 309-318, 2006.

Mah, E.L., Brinkworth, R.S., and O'Carroll, D.C. Bio-inspired analog circuitry model of insect photoreceptor cells. *Proc. SPIE Vol. 6036*, pp. 280-291, 2006.

Straw, A.D., Warrant, E.J., and O'Carroll, D.C. A 'bright zone' in male hoverfly (*Eristalis tenax*) eyes and associated faster motion detection and increased contrast sensitivity. *Journal of Experimental Biology* Vol. 209, pp. 4339-4354, 2006.

O'Carroll, D.C., Shoemaker, P.A, and Brinkworth, R.S.A. Bioinspired optical rotation sensor. *Proceedings SPIE*, vol. 6414, p. 641418, 2007.

Brinkworth, R.S.A., Mah, E.L., and O'Carroll, D.C. Pixel-wise adaptive imaging. *Proceedings SPIE* Vol. 6414, pp. 641418, 2007.

6. Interactions / Transitions

6.1. Participation/presentation at meetings, conferences, and seminars

Karin Nordström attended the Congress of the International Society for Neuroethology, 8-13 August 2004, Nyborg, Denmark.

David O'Carroll and Karin Nordström attended the International Congress of Entomology, 16-21 August 2004, Brisbane, Australia.

Patrick Shoemaker, David O'Carroll, and Karin Nordström attended the Workshop on Insect Sensors and Robotics, 23-26 August 2004, Brisbane, Australia.

Patrick Shoemaker, David O'Carroll, Steven Wiederman, and Paul Barnett attended the inaugural Queensland Brain Institute Workshop on Computational and Mathematical Neuroscience, 13-14 August 2006, Brisbane, Australia.

6.1.1. Conference Presentations / Posters Supported Directly by this Grant:

Nordström, K., O'Carroll, D.C. Small target motion detector neurons are present in female hoverflies. Proceedings of the Seventh Congress of the International Society for Neuroethology, Nyborg, Denmark, 8-13 August 2004.

Nordström, K., O'Carroll, D.C. Characterization of small target motion detection neurons of *Eristalis tenax*. Proceedings of the XXII International Congress of Entomology, Brisbane, Australia, 23-26 August 2004.

Nordström, K., Shoemaker, P.A. O'Carroll, D.C. Detection of small low-contrast targets across cluttered and moving backgrounds. Workshop on Insect Sensors and Robotics, Brisbane, Australia, 23-26 August 2004.

Nordström, K., and O'Carroll, D.C. Asymmetric receptive fields of target neurons in the dragonfly lobula. Society for Experimental Biology Annual Main Meeting 2005, Barcelona, Spain.

Shoemaker, P., Weiderman, S., and O'Carroll, D.C. Nonlinear neurons in the early visual ganglia of insects: new results and a computational model. Inaugural Queensland Brain Institute Workshop on Mathematical and Computational Neuroscience, 2006, Brisbane, Australia.

Weiderman, S., and O'Carroll, D.C. Modeling rectified transient neurons as inputs to correlation-type motion detection mechanisms. Inaugural Queensland Brain Institute Workshop on Mathematical and Computational Neuroscience, 2006, Brisbane, Australia.

Nordström, K., Barnett, P.D., and O'Carroll, D.C. Visual target detection in clutter. Australasian Society for the Study of Animal Behaviour Conference, 2006, Sydney, Australia.

6.1.2. Conference Presentations / Posters by the Principals in Related Areas:

Nordström, K., Swan, L., Mayrhofer, S., O'Carroll, D.C. Comparison of the image step response in flies and humans. Proceedings of the XXII International Congress of Entomology, Brisbane, Australia, 16-21 August 2004.

Shoemaker, P.A., O'Carroll, D.C. Silicon and abstract modeling of adaptive motion detection. Workshop on Insect Sensors and Robotics, Brisbane, Australia 23-26 August 2004.

O'Carroll, D.C., Shoemaker, P.A., Rainsford, T., Straw, A.D., Mah, E.L., Rajesh, S. Motion detection and velocity coding of natural scenes by the insect visual system. Workshop on Insect Sensors and Robotics, Brisbane, Australia, 23-26 August 2004.

Rainsford, T., O'Carroll, D.C. Pattern noise in neural coding of natural moving images. Workshop on Insect Sensors and Robotics, Brisbane, Australia, 23-26 August 2004.

O'Carroll, D.C., Rainsford, T., Mah, E.L., Rajesh, S. A 16-pixel yaw sensor based on insect motion detection. Workshop on Insect Sensors and Robotics, Brisbane, Australia, 23-26 August 2004.

Rajesh, S., O'Carroll, D.C. Elaborated Reichardt models for the detection of optical flow. Workshop on Insect Sensors and Robotics, Brisbane, Australia, 23-26 August 2004.

Mah, E.L., O'Carroll, D.C. Implementation of biomimetic models for adaptive photoreceptors based on insect neurobiology. Workshop on Insect Sensors and Robotics, Brisbane, Australia, 23-26 August 2004.

Dowd, L.M., Ali, I., Straw, A.D., O'Carroll, D.C. Interfacing VisionEgg-based stimulus generators for testing responses of biological and artificial vision systems. Workshop on Insect Sensors and Robotics, Brisbane, Australia, 23-26 August 2004.

Moyer de Miguel, I., Nordström, K., O'Carroll, D.C. Local motion adaptation in insect visual systems. Society for Experimental Biology Annual Main Meeting, Barcelona, Spain, 2005.

6.1.3. Participation in Seminars and Laboratory Meetings

Electrophysiology of *Eristalis* target neurons. Talk given at Department of Zoology, University of Cambridge, UK, by K. Nordström, 2005.

Sexual dimorphism of hoverfly target detection. Talk given at Department of Neuroscience, School of Biology, University of Bielefeld, Germany, by K. Nordström, 2005.

Hoverfly detection of small targets. Talk given at Visual Sciences, Research School of Biological Sciences, Australian National University, by K. Nordström, 2005.

Hoverfly motion vision. Talk given at Nobel Institute for Neurophysiology, Karolinska Institute, Sweden, by K. Nordström, 2005.

Motion vision in hoverflies. Talk given at Department of Neuroscience, Uppsala University, Sweden, K. Nordström, 2005.

Motion vision during flight - exciting new hoverfly findings. Talk given at Discipline of Physiology, The University of Adelaide, K. Nordström, 2005.

Rectifying transient cell model. Talk given at Discipline of Physiology, The University of Adelaide, S. Wiederman, 2006.

Insect visual motion detection and autonomous navigation. Talk given at Discipline of Physiology, The University of Adelaide, P. Shoemaker, 2007.

Analysis of neural bistability and amplification mediated by NMDA receptors. Talk given at the Laboratory for Neural Computation, The University of Southern California, P. Shoemaker, 2007.

6.1.4. Other

In an agreement with the DARPA/Lincoln Laboratory 3D-IC program managers, Patrick Shoemaker developed technology files (including layout setup, connectivity rules, and basic design rules) for the 3DM2 process in the Tanner Research IC design tool suite, in exchange for no-cost access to a DARPA-sponsored 3D IC fabrication run. These files and associated documentation were made available to the program managers and to other participants in the program who used Tanner tools on their projects, including R. Lovejoy at Sandia National Labs, J. Osborn at the Aerospace Corporation, A. Andreou at Johns Hopkins University, M. Zalalutdinov at NRL, and the faculty and staff at North Carolina State University who produced the primary tool suite for the process. Shoemaker assisted these participants with technology file installation and use, and incorporated feedback in revisions of the files during the course of the design phase.

In addition, Shoemaker consulted with E. Culurciello of Yale University, who kindly provided design guidance for the fabrication of photodetectors in the thin-film silicon-on-insulator 3DM2 technology.

6.2. Consultative and advisory functions

Patrick Shoemaker is serving as a co-advisor on the Ph.D. of Steven Wiederman at the University of Adelaide.

6.3. Transitions

As a result of work under this grant, Karin Nordström secured a Fellowship via the Swedish Research Council, which from 31 January 2005 has paid a large part of her salary. This freed up resources to pay Lachlan Dowd for programming support to the project.

Tanner Research was awarded two Phase I SBIR contracts, Navy contract N68335-06-C-0211 and Air Force contract FA8651-06-M-0203, and a follow-on Air Force Phase II contract, FA8651-07-C-0099. These deal with applications of wide-field visual motion detection, but have made use of models developed under support of the present grant (specifically, using rectifying transient cell models as drivers for motion adaptation).

7. New Discoveries, Inventions, or Patent Disclosures

The discovery of STMD neurons in female hoverflies by Nordström and O'Carroll was a novel finding, leading to publication of a paper in the Proceedings of the Royal Society of London.

An (apparently) novel semiconductor device, a dual complementary channel MOS transistor realizable in silicon-on-insulator technology, was conceived by Shoemaker and placed on the DARPA-sponsored 3DM2 run by Lincoln Laboratories. Due to delay in completion of this run, the circuit is not available for test and evaluation before the termination of the grant; characterization and a literature survey for similar inventions will take place in subsequent efforts.

8. Honors / Awards

For travel to conferences and foreign laboratories, Karin Nordström received a School ECR travel award, a Health Sciences Travel award, and an Oxford Gordon Conference travel award during the grant.

References

T.J. Bartolac, P.L. McCarley, "Detecting low-contrast moving point targets", *Proceedings of SPIE, Signal and Data Processing of Small Targets*, August 2003, Vol. 5204, pp. 41-50.

N. M. Jansonius and J. H. Van Hateren, "Fast Temporal Adaptation of on-Off Units in the 1st Optic Chiasm of the Blowfly,, *J Comp Physiol A*, vol. 168, pp. 631-637, 1991.

N. M. Jansonius and J. H. Van Hateren, "On-Off Units in the 1st Optic Chiasm of the Blowfly .2. Spatial Properties", *J Comp Physiol A*, vol. 172, pp. 467-471, 1993.

D. Osorio, "The Temporal Properties of Nonlinear, Transient Cells in the Locust Medulla", *J Comp Physiol A*, vol. 161, pp. 431-440, 1987.

M. Sarakaya, W. Wang, and H. Ögmen, "Neural network model of on-off units in the fly visual system: simulations of dynamic behavior", *Biological Cybernetics* Vol. 78, pp. 399-412, 1998